AGSO
AUSTRALIAN GEOLOGICAL SURVEY ORGANISATION

Collaborative MIM/AGSO Research Project:

BASE METAL MINERALISATION AT McARTHUR RIVER

STRUCTURE AND KINEMATICS OF THE HYC-COOLEY ZONE AT McARTHUR RIVER

1995/5

Mark Hinman
Australian Geological Survey Organisation
Canberra. ACT
June, 1993.
Revised January, 1995.

Division of Regional Geology and Minerals.

DEPARTMENT OF PRIMARY INDUSTRIES AND ENERGY

Minister for Resources: Hon. David Beddall, MP
Secretary: Greg Taylor

AUSTRALIAN GEOLOGICAL SURVEY ORGANISATION

Executive Director: Neil Williams

ISSN: 1039-0073
ISBN: 0 642 22330 0

SUMMARY AND CONCLUSIONS

This report summarises the results of a structural study on diamond drillcore (some oriented) and some surface and underground exposure at the HYC Pb-Zn(-Cu) mine at McArthur River, Northern Territory. The following main observations are relevant to the tectonic history of concurrent sedimentation, deformation and hydrothermal metal introduction at HYC-Cooley.

1. The Barney Creek Formation pyritic and mineralised shales at HYC contain distinctive drillcore-scale structures reflecting layer parallel compression and extension associated with predominantly "Top-to-NE" (and secondarily "Top-to-SW" layer-parallel movements). These structures, at the drillcore scale of observation, postdate diagenetic pyrite and concretions and finely laminated Pb-Zn ore and predate the Cooley inversion folding, thrusting and reverse faulting. They are interpreted to be syn-diagenetic; forming in a compacting and probably seismically active sediment pile composed of relatively brittle crusts, concretions, laminated pyrite and Pb-Zn ore interlayered with semi-consolidated (actively compacting), dolomitic-bituminous silts and muds which fail in a ductile fashion within a rapidly and inhomogeneously subsiding (NE tilting) sedimentary wedge. The kinematically "Top-to-SW" structures are probably produced during later SW-directed thrusting during the second kinematic phase of the "Cooley Inversion". The proposed NE tilting of the HYC portion of the Barney Creek shales is consistent with the known distribution of thickened sedimentary breccia accumulation (reflecting most rapid subsidence) in the NE.

2. The "Cooley Zone" at HYC is (half of) a transpressively inverted domain (positive flower structure) centred on the reactivated Emu Fault zone which contains the stratigraphically lowest units now in structurally highest positions. This inversion is believed to have culminated in upper HYC sedimentation time and probably produced a local source for the Upper Breccias. Two distinct kinematic phases characterise this inversion at Cooley: "Top-to-NW" followed by "Top-to-SW"; and are thought to be the local tectonic expressions at HYC of very broad scale regional transitions from an extended phase of extension controlling upper Tawallah Group to Barney Creek Formation deposition (Vic Wall, 1993) into the regionally extensive NS shortening event (Isan D1; ca 1600Ma). Onlap relationships north of HYC possibly involve condensed and atypical Upper Barney Creek Formation - Reward Dolomite sedimentation with high angle unconformity over reverse faulted, steeply dipping, brecciated and "Cooley mineralised" Mara Dolomite. If so, this would mark the end of the local "Cooley Zone" transpressive inversion.

3. The "Cooley Breccias" hosting copper (and lead) mineralisation are tectonic breccias lying along reverse faults within the overthrust block of Teena, Mitchell Yard and Mara Dolomites. The degree of fragmentation, fragment rotation and both dilation and stylolitic solution increases towards the reverse faults. It is unclear at present whether these breccias formed during both kinematic phases of transpressive inversion or only during the latter "Top-to-SW" phase (absence of oriented core in "Cooley Zone"). Pyrite and chalcopyrite are late in the "Cooley Breccia" infill paragenesis and within the footwall of the Basal Cooley Reverse Fault (at least) copper mineralisation is clearly associated with the latter "Top-to-SW" kinematic phase. Further detailed work on oriented core in the hangingwall breccias is planned.

CONTENTS

LIST OF ACCOMPANYING PLANS AND SECTION

N28-99	Plan Projection STRUCTURE	1:500
N28-99 Section 1.	GEOLOGY	1:500
	APPARENT DIP Overlay	1:500
	STRUCTURAL DATA Overlay	1:500
N28-99 Detail A.	Fold Axes & GEOLOGY	1:250
	Plan Projection STRUCTURE & APPARENT DIP Overlay	1:250
	STRUCTURAL DATA Overlay	1:250
N28-99 Detail B.	Fold Axes & GEOLOGY	1:250
	Plan Projection STRUCTURE & APPARENT DIP Overlay	1:250
	STRUCTURAL DATA Overlay	1:250
N28-99 Section 2.	GEOLOGY	1:500
	APPARENT DIP Overlay	1:500
	STRUCTURAL DATA Overlay	1:500
R29-05	GEOLOGY	1:500
	Maximum APPARENT DIP Overlay	1:500
29-05 Detail A.	GEOLOGY	1:100
	APPARENT DIP Overlay	1:100
	STRUCTURAL DATA Overlay	1:100
R29-05 Detail B.	GEOLOGY	1:20
	APPARENT DIP Overlay	1:20
	STRUCTURAL DATA Overlay	1:20
I22-55	GEOLOGY	1:500
	APPARENT DIP Overlay	1:500
	STRUCTURAL DATA Overlay	1:500
K22-55	GEOLOGY	1:500
	APPARENT DIP Overlay	1:500
	STRUCTURAL DATA Overlay	1:500

LEGEND (for all of the above)

LIST of FIGURES in Report

LIST of APPENDICES

ACKNOWLEDGMENTS

Many past and present MIMEX staff geologists produced the excellent and voluminous geological data base at HYC in the context of which this study has been undertaken. In particular, Matt Williams and Dugi Wilson had initiated work on the internal structure of the Cooley Zone after the observation of Vic Wall and Bill Perkins that a major reverse structure would explain the gross lithological relationships in the HYC-Cooley zone. Ross Logan has been very generous with his intimate and detailed knowledge of HYC. I thank Vic, Matt, Ross and Dugi for frank and open discussions of all aspects of McArthur and HYC geology. I also salute Joseph Janacek whose insightful work in the mid-1970's was clearly well ahead of his time.

AIMS of the MIM-AGSO COLLABORATIVE PROJECT

To use available HYC-Cooley drillcore, underground exposure in the exploration decline and outcrop mapping, where available:

- *to establish the gross geometry of the "Cooley Zone" in relation to the HYC Barney Creek stratigraphy with special emphasis on the distinction of the sedimentary and "Cooley" breccias.*

- *to resolve the structural-kinematic details of the "HYC-Cooley" zone and within this framework establish the relative timing of the stratiform Pb-Zn and the "Cooley-breccia" copper mineralisation.*

- *to establish a paragenetic sequence for the "Cooley-breccia" copper mineralisation to permit subsequent well-constrained fluid inclusion and geochemical work.*

- *to examine the microstructures common throughout the Barney Creek Formation in order to further constrain the timing of Pb-Zn mineralisation relative to sedimentation, diagenesis and the structural evolution of the hosting basin.*

INTRODUCTION

HYC and the McArthur River region are located in northern Australia within the Northern Territory on the eastern edge of the "Batten Trough" adjacent to the Emu Fault Zone (Fig. 1). The McArthur Region Geology is presented on Figure 1 and shows that the HYC deposit lies to the east of the NE-plunging Barney Hill anticline and immediately west of the Western Fault Block which is bounded to the east by the Emu Fault Zone containing horsts of Masterton Sandstone. The "Cooley Breccias" lie along the western edge of the Western Fault Block juxtaposed with the HYC sequence with unkown relationships that were the focus of this study.

The HYC-Cooley drillholes logged in this study are listed in Table 1 and located on Figure 2. Table 1 also indicates the holes that were quantitatively structurally logged, the orientation method applied and the detailed Plans and Sections that accompany this report.

DRILLCORE STRUCTURE

Principles and Assumptions

Structural information can be extracted from drillcore from surveyed drillholes provided the recovered core can be rotationally reoriented (ie. correctly rotationally positioned around the drillcore's axis). Two groups of methods exist to achieve this. The first involves the periodical physical marking of core before it is broken from the bottom of the hole and then the "fitting together" of all the drillcore between oriented pieces to provide a continuous reference line. Structural features of interest are then measured relative to this reference. The second method exploits the known orientation of one structural element to orient core from surveyed drillholes allowing other elements of interest to be measured.

Both orientation methods allow drillcore to be physically reoriented in space (using a sand bucket or core orientometer jig) which subsequently allows the direct compass measurement of the other elements of interest. However, such physical reorientations and measurements are laborious and time consuming, preventing the generation of large data sets. An alternative method involves the measurement of the **relative** orientation of structures with respect to either the core orientation mark or the known structural element without physically reorienting the core. The spatial orientations of structures can then be calculated within a spreadsheet (Hinman, 1993). The present study uses a spreadsheet, which is a modification of the one published by myself.

This study uses both principle methods of drillcore orientation. Within the main area of HYC Pb-Zn mineralisation most of the existing drillholes are subvertical and the drillcore unoriented. However, the local orientation of bedding is well constrained from detailed correlation between drillholes within the grid-drilled HYC evaluation area. Therefore, in individual holes, provided the drillhole has not been drilled normal to bedding, drillcore can be reoriented using the interpolated local bedding orientation. However, due to the natural variability in the dip and strike of bedding and the rigidity of the bedding orientation assumption, this derived structural data will have a scatter (error) of the same order as the natural variability of the bedding orientation.

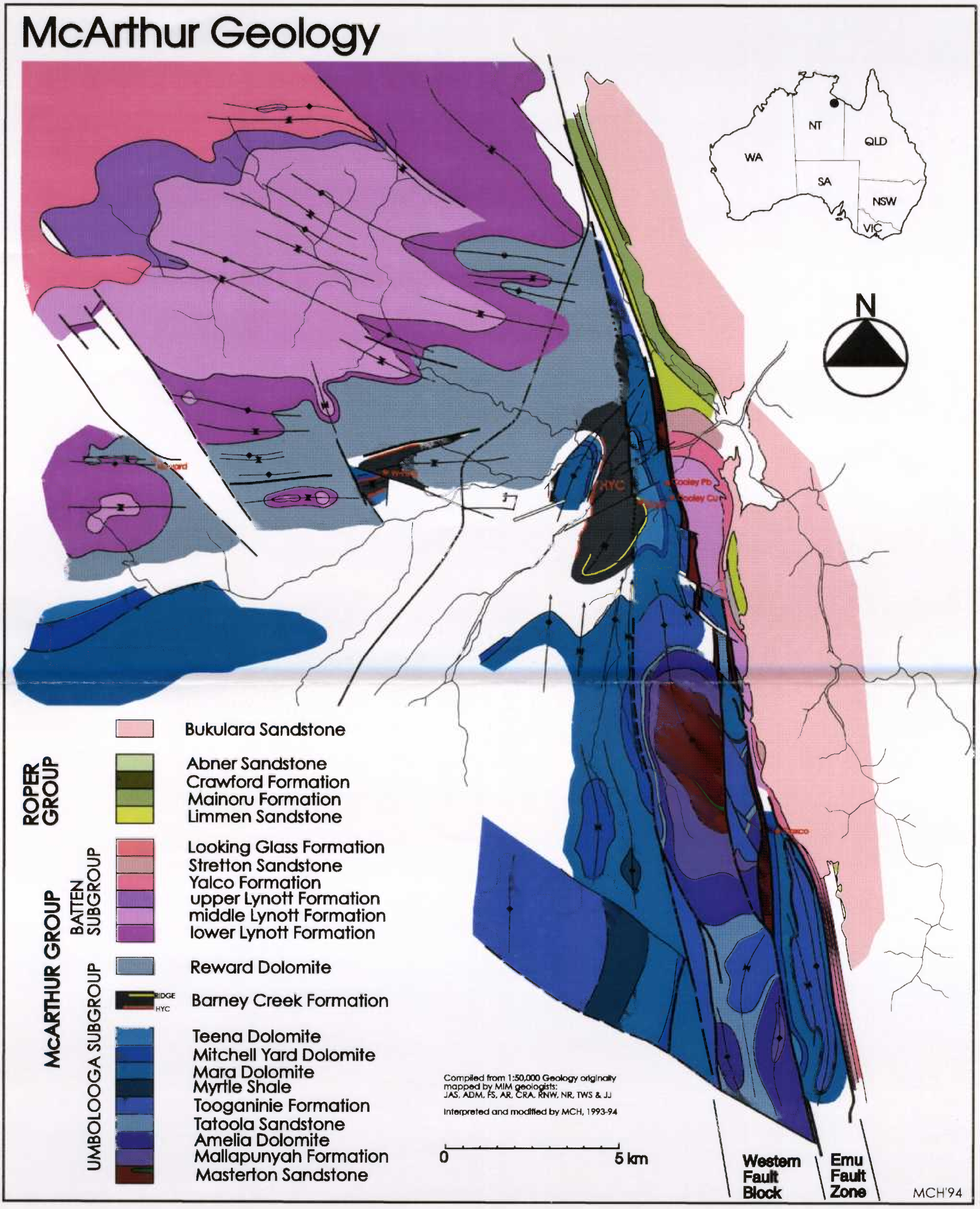

Figure 1. McArthur River Geology

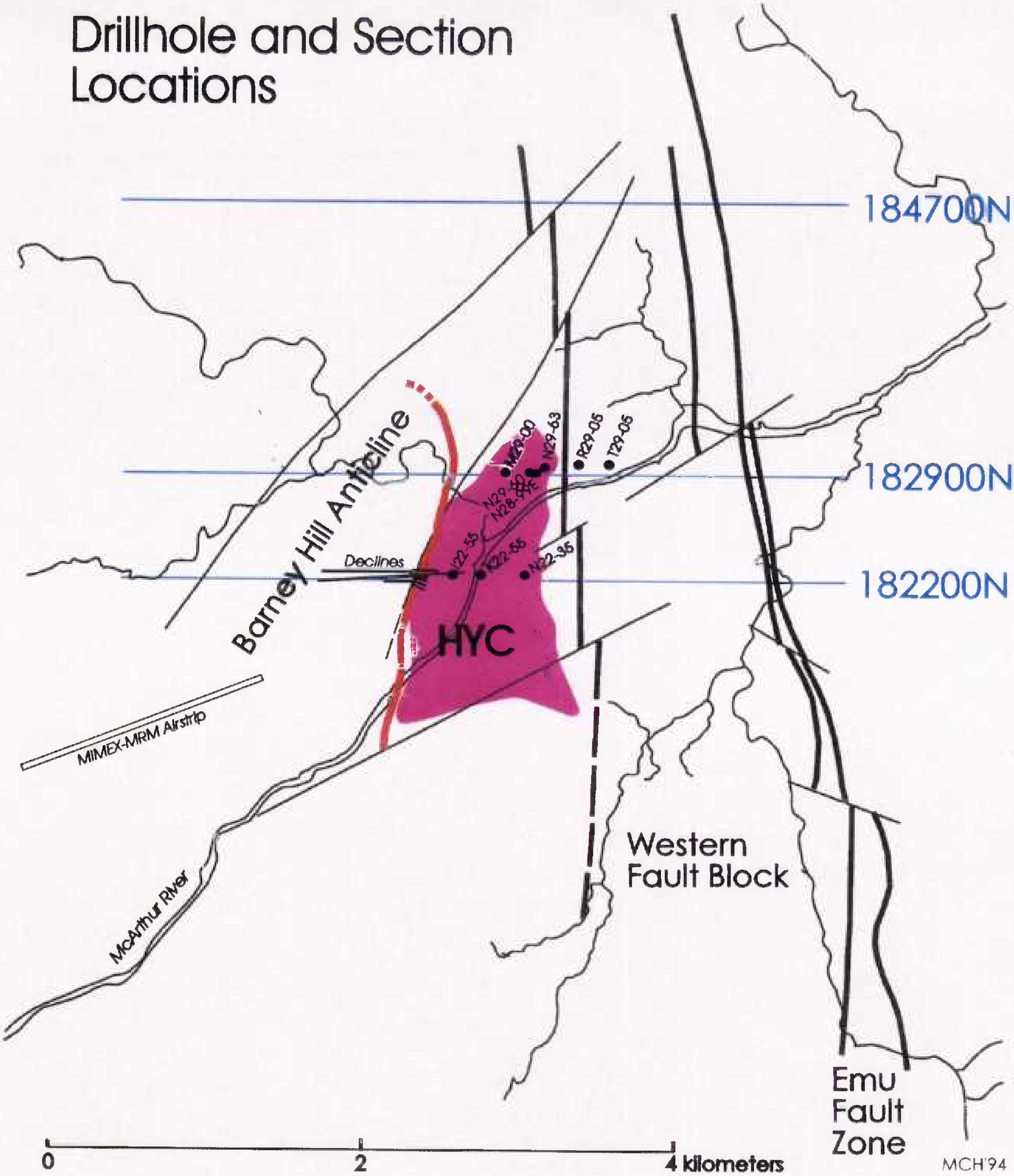

Figure 2. Location of Section and Drillholes at HYC

Along the eastern edge of the HYC Pb-Zn mineralisation and within the "Cooley Zone", where the gross geometries were uncertain and detailed structure unknown, fully oriented drillcore was required to resolve the geology, structure and kinematics. Once some of the aspects of the gross geometry, detailed structure and kinematics were resolved from the fully oriented drilling, measurements from long lengths of fitted-together drillcore from other vertical and unoriented drillholes could be iteratively manipulated within the spreadsheet (ie. rotated around their own drillhole axis) to produce "best fit" solutions. Fully oriented drillcore is only as good as the technique employed to orient the core and the care taken in the technique's execution. There is little point in attempting to recover oriented core to solve critical problems if the confidence in the technique and its application is low (see **Limitations** below).

Table 1. Drillholes logged in this Study

		STRUCTURAL		
Hole	Section	Orientation Method	Data Status	Plans/Section Plotted and Provided
I22-55	182200N	Bedding	Finalised	1:500
K22-55	182200N	Bedding	Finalised	1:500
N22-35	182200N	Bedding	1°Calc only	
N29-00	182900N			
N29-60	182900N			
N28-99E	182900N	Downhole Spear	Finalised	1:250,500,1000
O29-63	182900N			
R29-05	182900N	"Best Fit"	Finalised	1:20,100,500
T29-05	182900N		Max App Dip	
R27-05	182700N		Max App Dip	
Emu 16	184700N	Downhole Spear		
Mt Stubbs 3	184700N			
Mt Stubbs 4	184700N			

1. "Best Fit" of bedding, fault orientations and kinematic indicators with adjacent fully oriented drillhole and nearby outcrop.
2. MaxAppDip=Maximum Apparent Dip treatment only. Commonly core too broken to fit together large sections for iterative "Best Fitting".

Limitations

The resolution of structures and kinematics in drillcore has limitations. The major sources of these are, firstly functions of the drillcore orientation process and secondly, the relative scale of the observation (ie. core size) in comparison with the scale of the investigated structures.

The scatter in data derived from drillcore oriented according to rigid assumptions made about bedding orientations will reflect the natural variability in bedding dip and strike (see also above). Around fault zones where bedding is commonly rotated significantly the method completely fails (eg. I22-55). The only recourse is to attempt to fit all the core together from outside the disturbed zone into the fault zone....commonly a task made difficult, impossible and fruitless by the broken nature of core around the fault.

In drillholes where bottomhole orientations have been successfully done at regular intervals, the derived structural data should be excellent. Unfortunately, those methods that rely on gravity in inclined holes to mark the bottom side of recovered core are prone to considerable "bounce" off the back of the drill bit and/or the bottom of the core barrel at the bottom of the hole resulting in very significant misorientations. This becomes obvious when long sections of core through more than one core orientation mark can be successfully

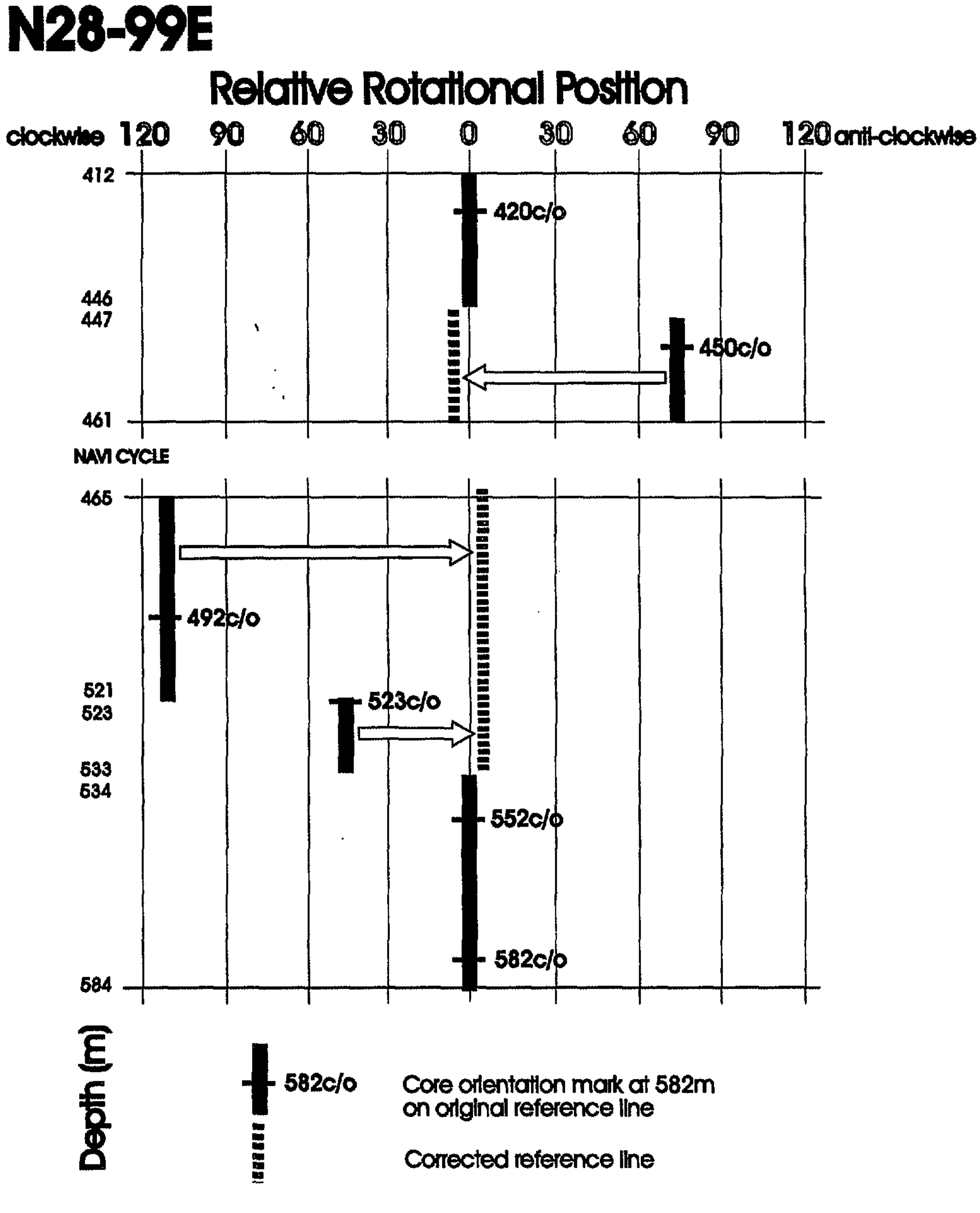

Figure 3. N28-99E Core Orientation - Relative Rational Positions

fitted together. Severe problems of this nature occurred in the critical hole, N28-99E between 412m and 584m (Fig. 3) with the result that confidence in the structure of this zone is considerably reduced. A little more care in the execution of the techniques and more regular orientation where ground is more broken can vastly improve the final structural product and improve the understanding of critical relationships and processes. Figure 3 shows how far successive core orientation marks were relatively rotated in two sections of completely fitted-together drillcore (separated by a Navi drilling cycle) in N28-99E between 412m and 584m. The figure also shows the final (version 5!) adjustments that were made, based largely on bedding orientation correlations across the Navi drilling gap and the "agreeing" core orientation marks at 552m and 582m. The most doubtful zone remains between 412m and 461m....a section that contains an abundance of interesting thrust? microstructures in W-Fold Shale.

The second problematic aspect of the resolution of structures from drillcore is scale dependant. Structures smaller than the size of the core (eg. microfaults, low angle microthrusts....) can commonly be fully resolved with respect to orientation and direction, sense and magnitude of movement when offsets are smaller than the intersection of the structure with the core. However, at the other end of the scale spectrum, drillcore through very large structures (eg. the Basal Cooley Reverse Fault) are composed of broad zones (many to tens of meters) of mixed lithologies, spaced anastomosing fabrics and abundant secondary structures. Orientation of the main structure, in these cases, is commonly impossible to determine from oriented drillcore in an individual hole. Multiple intersections of the structure are required to accurately resolve its orientation. Oddly, however, the gross direction and sense of movement can commonly be determined, although the magnitude of displacement is generally well beyond the scale of the core. Between these end members of scale there are many structures that can be variably resolved with respect to orientation and kinematics. It should be born in mind that, without multiple intersections, it is the larger structures that are less well constrained in orientation, despite being generally well understood kinematically from associated smaller scale secondary structures.

DETAILED STRUCTURE AND GEOLOGY

The detailed geology and structure of selected HYC and HYC-Cooley drillholes are presented in a series of plans, sections and overlays listed at the start of this report and summarised in Table 1. The structural logs are presented in spreadsheet form in Appendix I. There are two distinctive groups of structures observed in drillcore with contrasting orientations and kinematics. The earliest group of structures are confined to the W-Fold, Lower Dolomitic, HYC mineralised Lower Pyritic, Upper Pyritic, Bituminous and Upper Dolomitic Shales (Barney Creek Formation Shales) and are thought to have formed within the Barney Creek sediment pile while the sediments were still relatively unlithified. The second group of structures clearly affect the entire sequence and have been logged from Mara Dolomite as stratigraphically high as the Upper Breccias. These reverse movement structures reflect a local inversion that formed the, so called, "Western Fault Block" and "Cooley Zone".

Detailed structural work has been completed on two sections: 182200N and 182900N. Work on 182200N includes mapping of Barney Hill, mapping of the Exploration Decline and detailed, quantitative structural logging of I22-55, K22-55 and N22-35. Work on 182900N includes mapping of Barney Creek, mapping of the Barney Creek Crossing outcrops and detailed, quantitative structural logging of N29-99E, R29-05 and T29-05 (see 1:10000 Geology Plan). Qualitative structural observations were made in the other logged HYC-Cooley drillholes listed in Table 1.

"EARLY" (MICRO)STRUCTURES

The earliest, drillcore-scale, structures include the extensional "Step" Microfaults, "soft sediment" intraformational Microfolds and Imbricate Stacks, the Low Angle (to bedding)

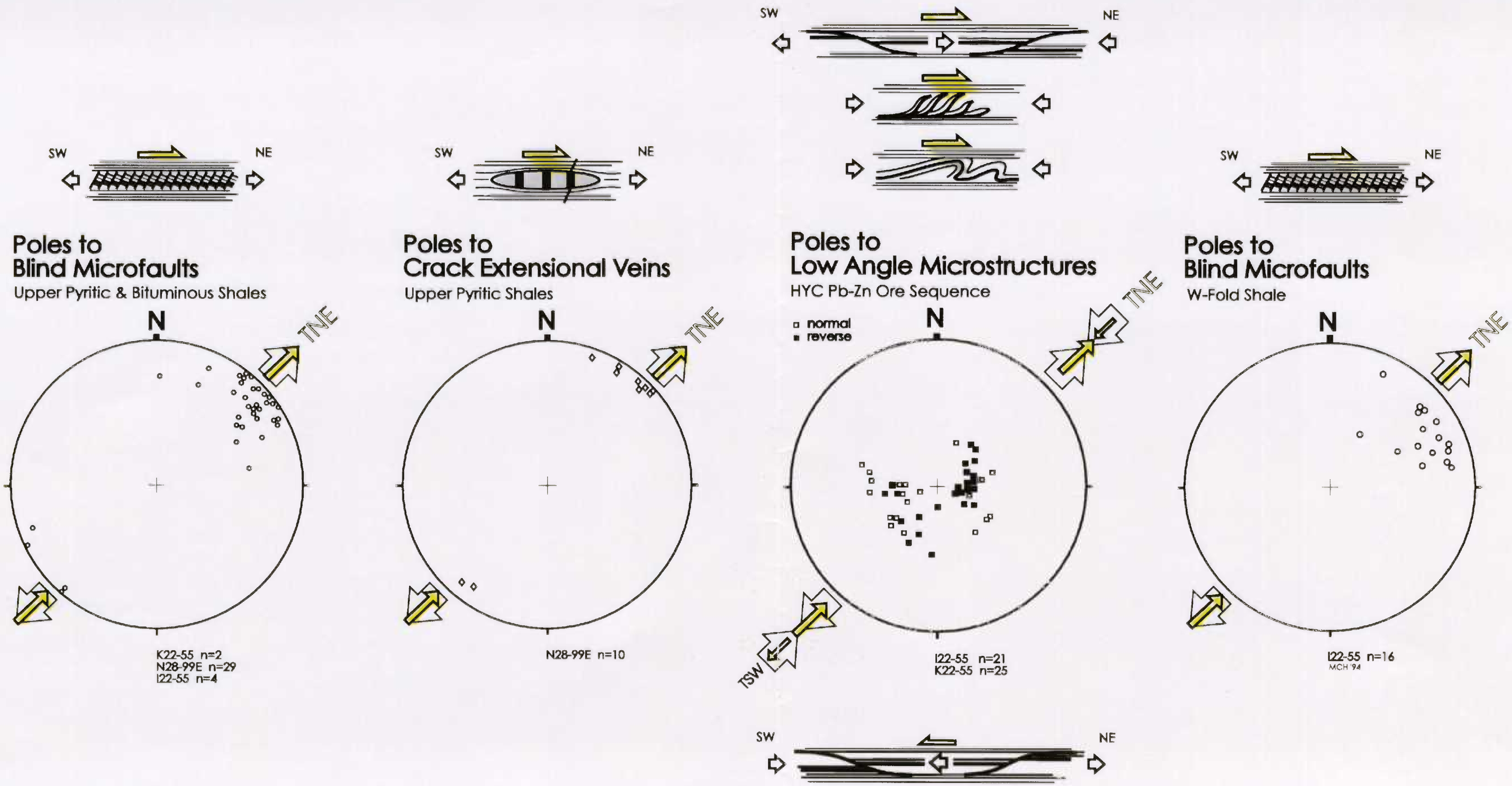

Figure 4. Structures and Representative Stereoplots of the Barney Creek Formation

Microfaults and Crack Extensional Veins in concretions. Sketches of these structures are shown on Figure 4. They have been structurally logged in I22-55, K22-55, N22-35 and N28-99E (see accompanying plans and sections and Appendix I). The most remarkable feature of all these structures is their consistent strike and kinematic indication (bar one set of low angle structures; see below). Representative stereoplots of these structures are also shown in Figure 4 and show that, within the tolerances of the drillcore orientation method used (see Table 1), these structures strike NW-SE.

Microfaults and Extensional Veins....."Top-to-NE"

The extensional Microfaults are very common throughout the W-Fold Shale and the Pyritic and Bituminous Shales. The Crack Extensional Veins are confined to concretionary sections of the same units and are commonly continuous with moderate scale Microfaults. The Microfaults display a continuum of scales from very closely spaced faults displacing a small number of laminations and apparently confined to those set of laminations by bedding parallel slip on adjacent layers, up to larger, similarly oriented, faults cutting many centimetres to tens of centimetres of laminations including bands of the smaller scale Microfaults. They all show "SW-Block-Down" displacements and indicate layer-parallel extension. However, the bedding-confined, smallest scale Microfaults are difficult to rationalise with "SW-Block-Down" normal block faulting as they are "rootless". They are better rationalised by (and consistent with) "Top-to-NE" bedding parallel slip. The larger scale Microfaults are therefore likely to reflect similar bedding-parallel deformation but on thicker packages. The Extensional Veins in concretions are intimately associated with Microfaults and indicate NE-directed layer-parallel extension.

Imbrication and Intrafolial Folds....."Top-to-NE"

These moderately common structures occur within the Mineralised and more highly Pyritic Shales. Where they have been measured they too are consistent with "Top-to-NE" layer parallel deformation but reflect layer-parallel compression.

Low Angle Microstructures....."Top-to-NE & Top-to-SW"

The Low Angle Microstructures are extremely common within the Mineralised Shales and moderately so within highly Pyritic Shales. They usually lie at 20-30° to bedding regardless of the orientation of bedding and flatten out into bedding (Fig. 4). They clearly displace bedding laminations by fractions to a few millimetres, and they display both normal and reverse movements. Measurements in a number of holes (I22-55, K22-55, N22-35, N28-99E) suggest that NE-dipping NORMAL and SW-dipping REVERSE Low Angle Structures, indicating "Top-to-NE" layer-parallel deformation, are roughly equally common and together are considerably more common than SW-dipping NORMAL and NE-dipping REVERSE Low Angle Structures that indicate "Top-to-SW" layer-parallel deformation (see Fig. 4). Together they represent conjugate sets of layer parallel compressional and extensional structures reflecting dominantly "Top-to-NE" and secondarily "Top-to-SW" (or "Bottom-to-NE") kinematics (see extensional and compressional arrows on Fig. 4).

Relative Timing Relationships

Some of the relative timings of the above structures with respect to each other and with respect to syn-diagenetic features (eg. pyrite, concretions and ?Pb-Zn mineralization) are evident from overprinting relationships. Following are a number of timing observations, which are summarised in Figure 5:

R9500506

a) Medium to large scale Microfaults cut concretions, Intrafolial Folds, Imbricate Stacks, small scale Microfaults and rarely Low Angle Microstructures (Microfaults are rare within Mineralised Shales).

b) Extensional Veins and associated Microfaults cut concretions.

c) At the drillcore scale of observation, all the microstructures cut and/or deform early diagenetic pyritic laminae and Pb-Zn mineralised shale laminae.

d) Low angle REVERSE structures cut and displace Low angle NORMAL structures as often as vice-versa.

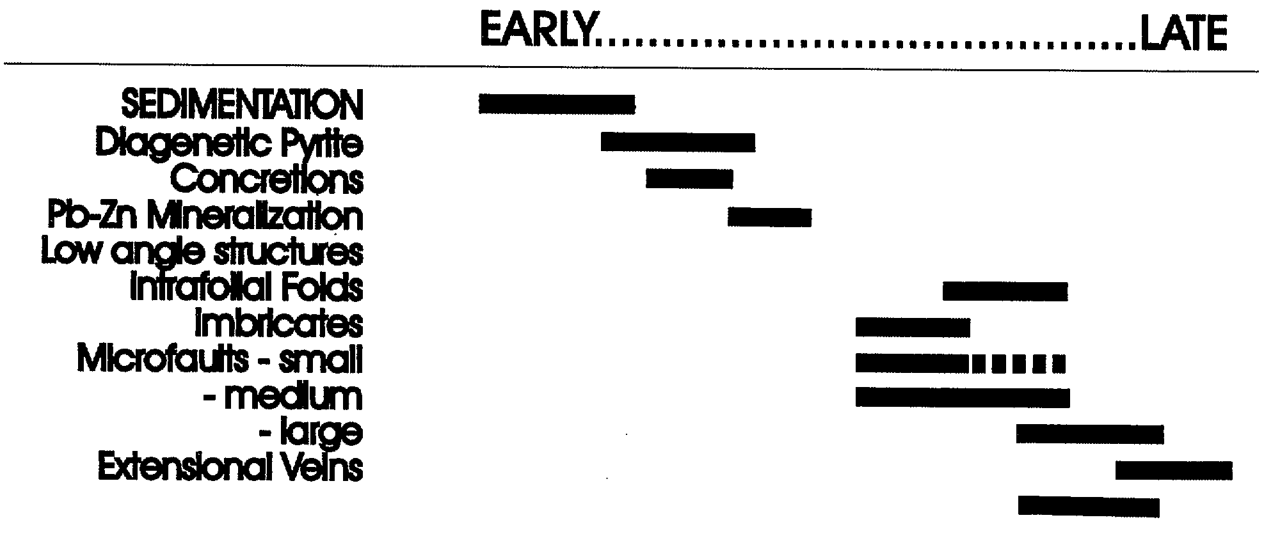

Figure 5. Relative Timing of Early Structures and Diagnetic Features within an individual horizon

"LATE" TRANSPRESSIVE STRUCTURES

A number of major fault zones whose gross orientations and kinematics are not easily resolved from drillcore (see Limitations in DRILLCORE STRUCTURE above) are present in drilling towards the eastern edge of the HYC Pb-Zn mineralised area and within the "Western Fault Block" or "Cooley Zone". Fortunately, on the major section logged, 182900N (Figs 6 & 7), the drillhole spacing is sufficiently close to constrain the gross geometry of these major structures. In addition, a host of secondary, parallel and conjugate structures associated with the major structures are fully resolvable with respect to orientation and kinematics. They can be used to further constrain the orientation of the major structures assuming a degree of parallelism between the different scale structures and fully resolve the large scale kinematics.

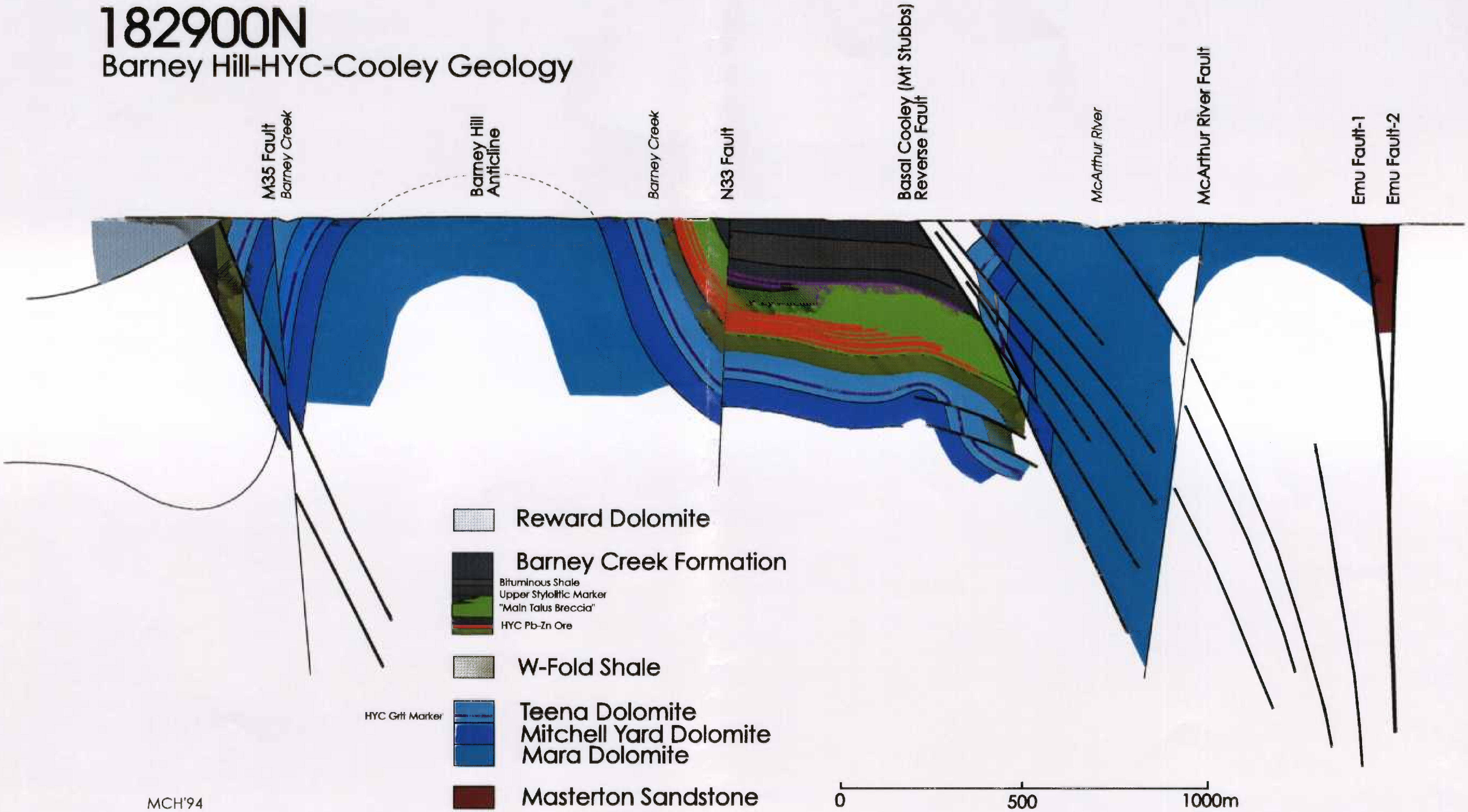

Figure 6. Section 182900N Geology

Gross Geometry of Cross Section 182900N

The interpreted gross geometry across the HYC-Cooley zone at 182900N is presented in an accompanying Section (Fig. 7) and Structural Overlay (Fig. 8). The Cooley Zone is interpreted to be a transpressively reverse faulted, steeply dipping (to locally overturned), short limb block of folded Teena, Mitchell Yard and Mara Dolomite lithologies (on this section) thrust against and over much of the Barney Creek Formation.

The Basal Cooley Reverse Fault was intersected in R29-05 and is a 5 meter wide anastomosing zone of mixed rock types from above (Teena) and below (Shale ±pyritic and sedimentary breccia-grits). The orientation of this structure is constrained by the geology of the drillholes adjacent to R29-05. The structure may be steeper than indicated on Figures 6 and 7 but must be a *reverse fault*. The structures within the hanging wall of the basal reverse fault are most commonly zones of intense tectonic brecciation containing rotated fragments of the adjacent dolomitic lithology. The zones of intense brecciation separate blocks of differently, but internally consistently oriented, coherent dolomitic stratigraphy. They have been represented on the section, for convenience, as reverse faults (F3; 182900N; Fig. 7) although only a few actually contain a discrete structural surface that can be measured (Fig. 8). Based on the bedding orientations (Maximum Apparent Dips; ie. rotationally unfixed core; see Table 1) and consistent facings (ie. uphole or downhole) within coherent blocks in R29-05 and T29-05, some attempt to schematically link the zones of intense brecciation has been made on Figures 6 and 7. Very steep to overturned (downhole facing) sections are present in both holes and have been tentatively correlated. However, it seems highly likely that these zones of intense brecciation and faulting anastomose more strongly than indicated and limited structural data, where fault surfaces have been measured, suggest that the structures within the hanging wall of the Basal Cooley Reverse Fault are not parallel to the Basal Fault and infact strike at moderate angles to it.

In the footwall of the Basal Cooley Reverse Fault are a number of flat to gently NE dipping thrust surfaces (F2; 182900N; Fig. 7) that within the W-fold Shale, Lower Pyritic Shales (& sedimentary breccias) and Main Talus Breccias are probably bedding parallel (NE dipping) and exploit the shaly (weak) horizons within the HYC package.

HYC Ore-Sedimentary Breccia Facies Relationships

At the eastern end of Section 182900N west of the "Cooley Zone" the sedimentary breccia cycles of the HYC Mineralised Shale and Main Talus Breccia can be well correlated through a number of drillholes (N29-60, O29-63 and N28-99E; Figs 6 & 7). From west to east Orebodies 8 to 5 are progressively displaced in the sedimentary pile by breccia cycles. Orebodies 4 to 2 are significantly less mineralised in their easternmost intersections (N28-99E) where the Basal Breccia, the strongly pyritic units at 2 Orebody and above 3 Orebody, the 2/3 interore breccia cycle and the base of 4 breccia cycle are well correlated across the entire section.

The breccias at 5 to 8 Orebody positions are (galena) mineralised. Both the sedimentary breccia matrix and the rims of dolomitic clasts commonly show partial galena replacement. This mineralisation is quite unlike the "Cooley Brecciation" style of mineralisation found further east on this section in the footwall of the Basal Cooley Reverse Fault (R29-05) where base metals are localised within fracture networks within the breccia clasts (Fig. 8). It seems probable that three mineralisation styles exist on this section. Temporally the first two involve ?syn-diagenetic replacement of sedimentary breccia clasts (and matrix) while, to the west, the main HYC Pb-Zn orebodies formed by ?replacement of fine grained sediments which were deposited in onlapping positions with respect to non interore

Structural Summary OVERLAY Key

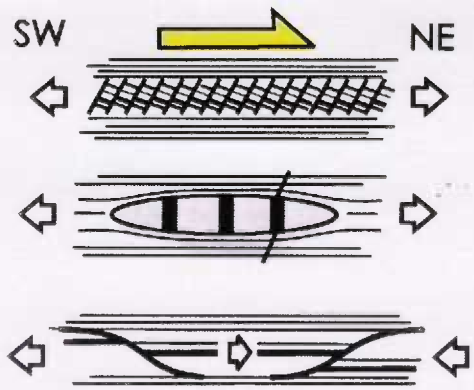

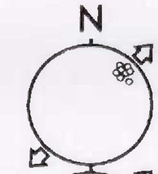

"Top-to-NE"

∘ poles to microfaults

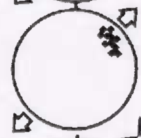

"Top-to-NE"

• poles to extensional veins

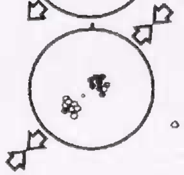

"Top-to-NE"
("Top-to-SW")

∘ • poles to normal/reverse faults

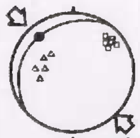

"Top-to-NW"

▫ poles to fold axes
▵ poles to cleavage
• thrust slickensides

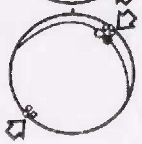

"Top-to-SW"

∘ poles to extensional veins
• ∘ thrust/bedding slickensides

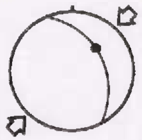

"Top-to-SW"

• reverse fault slickensides

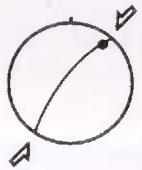

"West-to-S & UP"

• fault slickensides

(1a) Microfaults

(1b) Extensional Veins

(1c) Low angle Microstructures

(2a) Shallow Thrusts

(2b) Shallow Thrusts

(3b) Reverse Faults

(4) Late Steep Faults

182900N
Structural Summary
OVERLAY

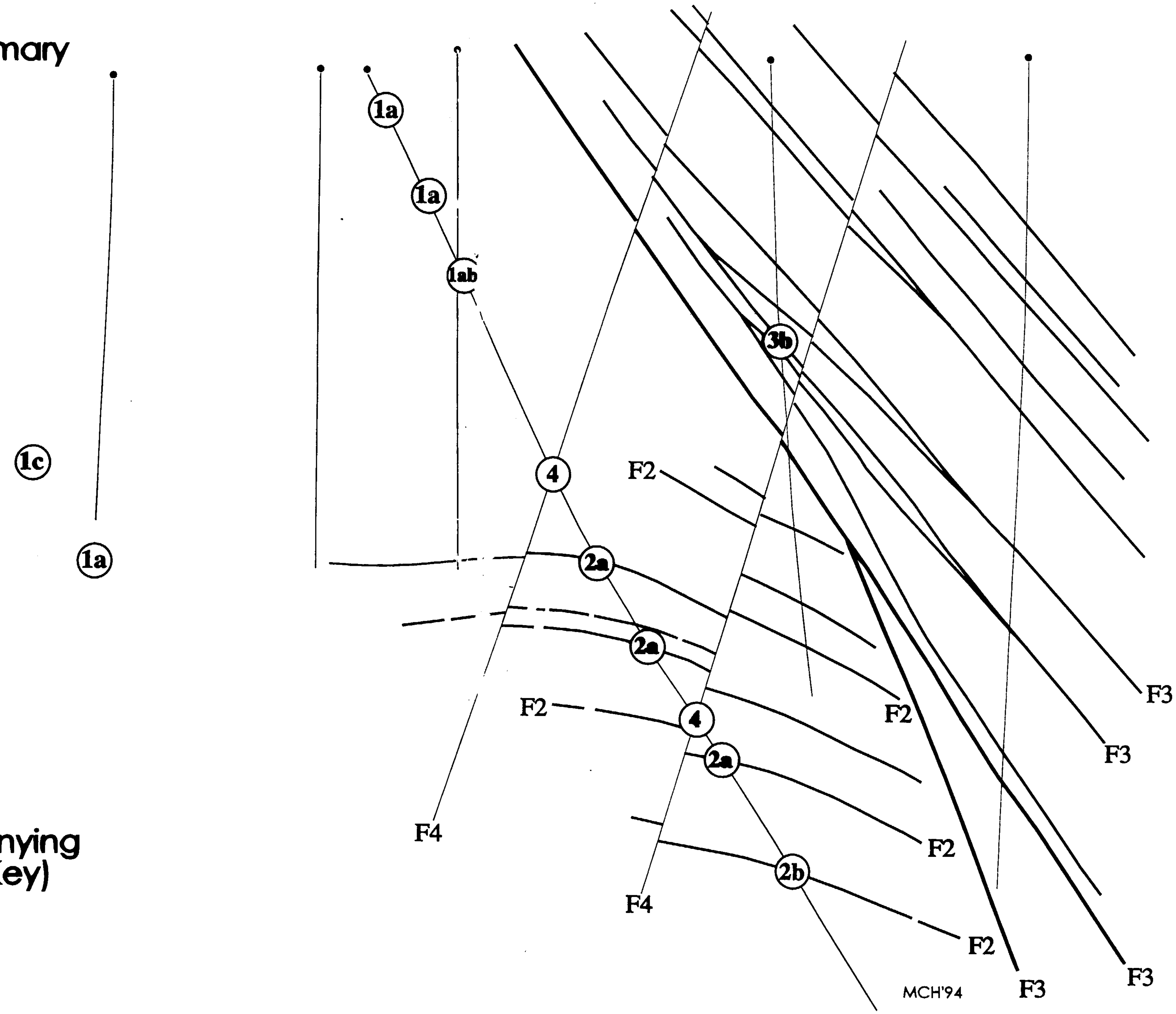

(see accompanying OVERLAY Key)

Figure 8. Structure Summary Overlay

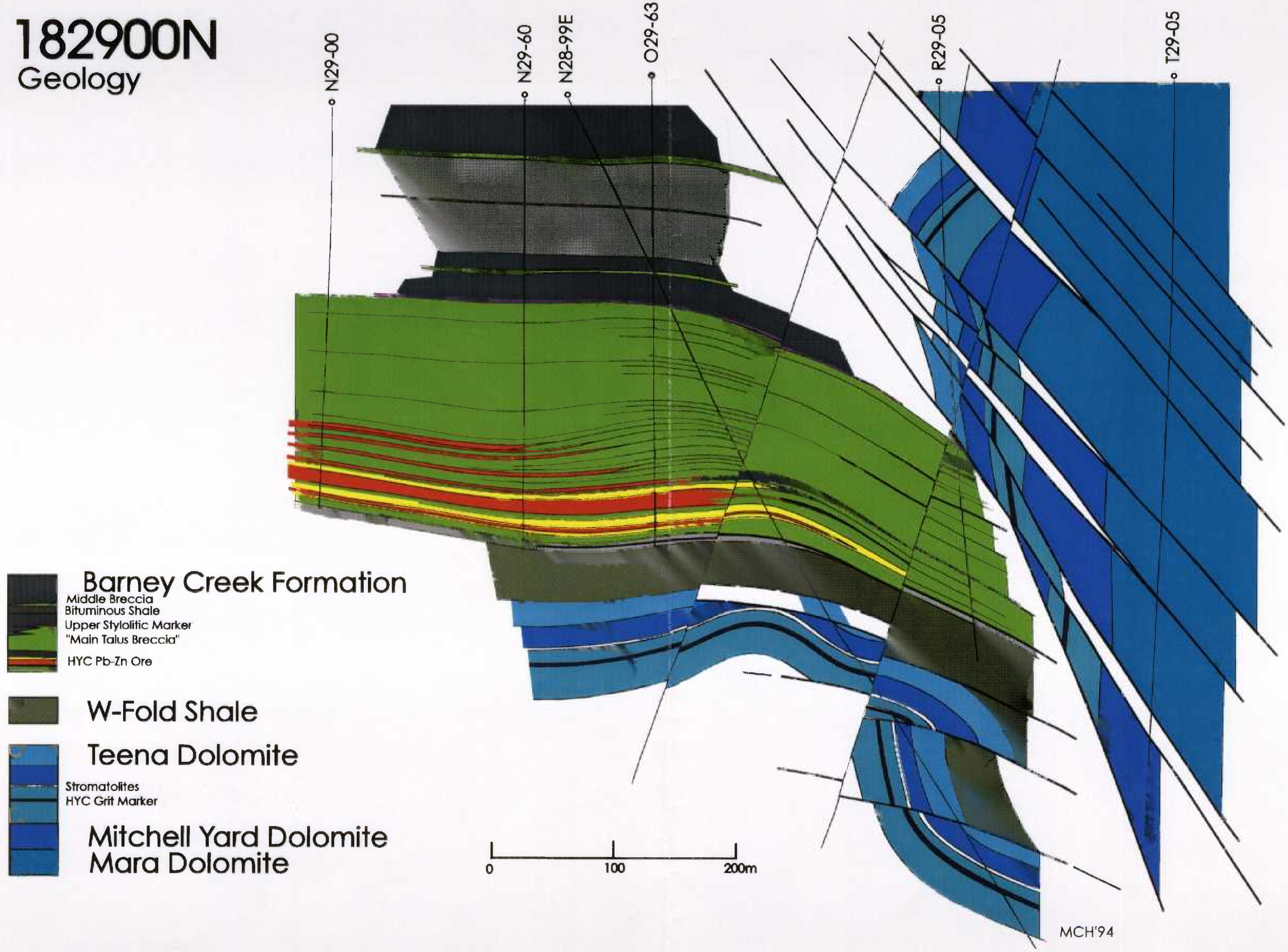

Figure 7. 182900N HYC-Cooley Geology

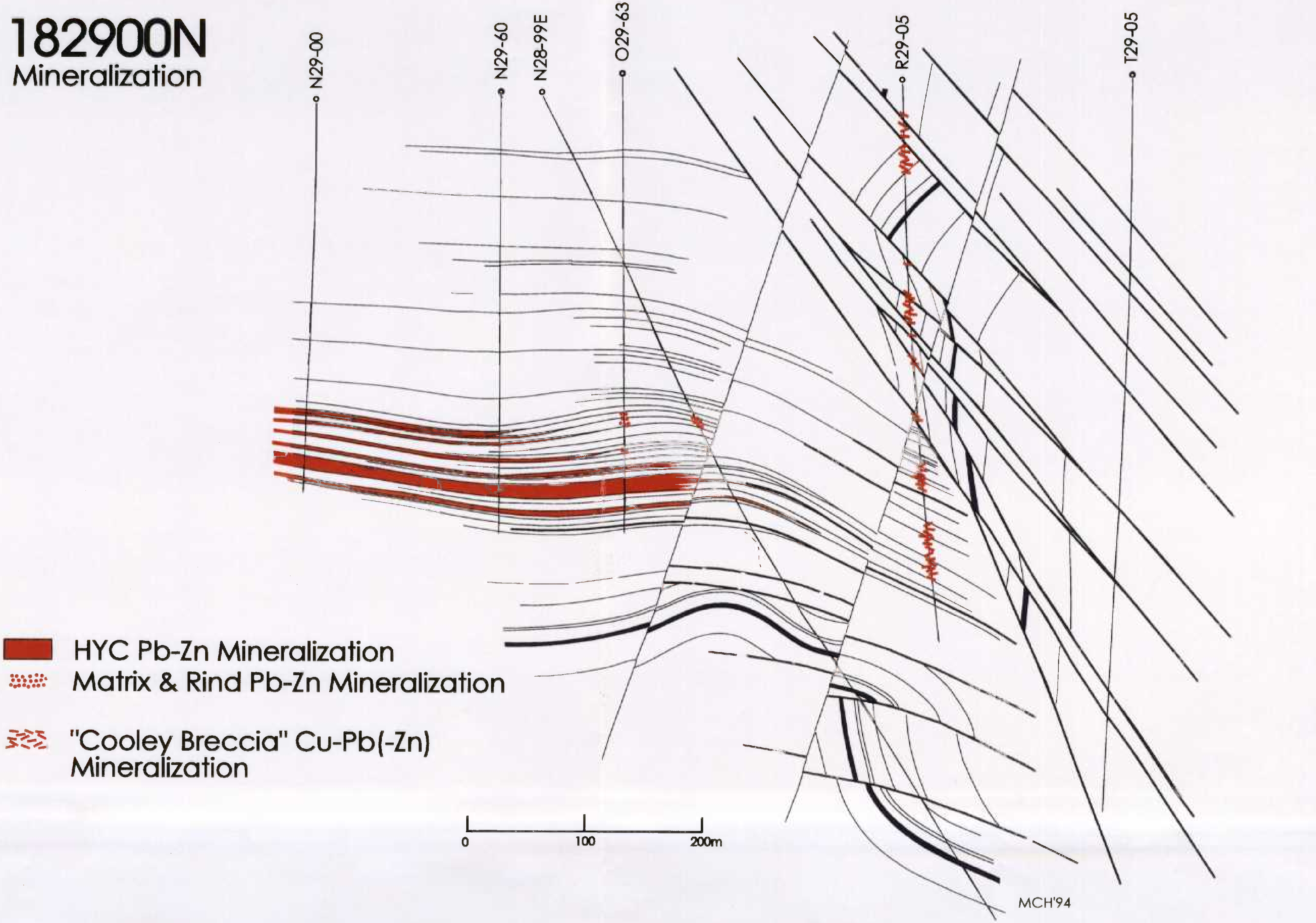

Figure 9. 182900N Mineralisation Styles

sedimentary breccia cycles. The interore breccia cycles are continuous from west to east where they are sharply truncated by the Basal Cooley Reverse Fault. The third style is the "Cooley Breccia" mineralisation in both the footwall and hangingwall of the Basal Cooley Reverse Fault and is related to the later transpressive inversion event (see below).

Kinematics in the "Cooley Zone"....."Top-to-NW" and "Top-to-SW"

The kinematics of this complex zone between "normal" HYC Barney Creek stratigraphy and the overthrust "Cooley brecciated" Western Fault Block is best resolved from the oriented drillhole N28-99E. The detailed structural data and kinematic indicators are presented in the accompanying N28-99E 1:500 and 1:250 scale Structural Overlays and summarised on the 182900N Structural Overlay (Figs 7 & 8).

The major tectonic and kinematic indicators resolvable in drillcore are:

Cleavage	normal to a shortening direction
Fold Axes	normal to a plane containing a shortening direction
Slickensides	indicating direction of movement on fault and bedding planes
Extensional Veins	indicating direction and sense of movement when associated with planar failure

These indicators suggest two distinct shortening directions and failure movement directions on the shallowly dipping thrust planes (F2) and also (probably; see below) on the steeper reverse fault planes (F3).

Small scale folding (tens of centimetres to a few tens of meters wavelengths), associated with either (pre-failure) shortening or with planes of failure, and slickensides on shallow thrust surfaces at all scales suggest a phase of approximate *SE-NW shortening* with *"Top-to-NW"* movements where failure has occurred. Some slickensides on bedding within the Upper Pyritic and Bituminous Shales are consistent with this kinematic phase and are the only known (at present) expression of this inversion deformation in these units. Other structures that are probably associated with this phase of shortening are the Barney Hill anticline and a parasitic syncline-anticline pair at the base of the exploration decline. A recumbent syncline-anticline pair within the lower Pb-Zn orebodies along the eastern edge of the HYC ore block in the immediate footwall of the Basal Cooley Reverse Fault has a parallel trend in the northern half of the HYC ore block but has a more NNW-SSE trend to the south possibly reflecting the adjacent orientation of the Basal Cooley Reverse Fault there.

A crude macroscopic cleavage is visible within the dolomitic shales in N28-99E where a broad anticlinal arch exists within the lower Mineralised Shales in the footwall of the Basal Cooley Reverse Fault. The poles to cleavage here are fairly scattered, probably as a result of post-cleavage fault related rotation, but suggest a 50-70° east dipping fabric sub-parallel with the Basal Cooley Reverse Fault and consistent with a strong component of E-W shortening adjacent to the transpressively failed Basal Cooley Reverse Fault.

The second phase of this transpressive inversion is expressed by another distinct set of slickensides on shallow thrusts and bedding in the footwall of the Basal Cooley Reverse Fault and reverse faults in its hangingwall (a few that have been resolved). These are consistent with *NE-SW shortening.* Extensional veins at high angles to planes of failure associated with this shortening episode and measurable displacements indicate *"Top-to-SW"* senses of movement.

There are no diagnostic overprinting relationships observed in drillcore to fix the relative timing of these two kinematic phases of transpressive deformation responsible for the formation of the "Cooley Zone". The most logical sequence, however, would have initial SE-NW shortening folding the sequence and associated locally with and culminating in kinematically consistent ("Top-to-NW") failures followed later by the distinctively different phase of "Top-to-SW" failures. It is unclear (at present) whether the overthrusting of the lower dolomitic stratigraphy over the upper HYC stratigraphy initiated at the earlier SE-NW stage or was confined to the later NE-SW kinematic phase. However, it seems probable that the major macroscopic structures (Barney Hill anticline and associated decline folds, major folds centred within the Western Fault Block; Fig. 6) formed during the earlier SE-NW shortening episode. These progressively developed steep to overturned west limbs that then failed transpressively with "Top-to-NW" kinematics, resulting in the reverse fault juxtapositioning of the steeply-dipping, dolomitic Western Fault Block and the shallow-dipping, HYC pyritic shale sequence across the Basal Cooley Reverse Fault. Subsequent NE-SW shortening would have reactivated the Basal Cooley Reverse Fault and other existing footwall thrusts and faults but appears to have generated new structures in the hangingwall. "Top-to-SW" failures have been resolved by "best fit" methods in the overthrust block associated with "Cooley Brecciation" (see below) but the level of data does not preclude some effects of the earlier kinematic failure phase in this zone. Note, however, that SW bedding dips in outcropping Cooley Breccias are more compatible with reverse faulting and overthrusting of folded, NE-dipping lower Barney Creek Formation and underlying dolomitic stratigraphy during NE-SW shortening.

Cooley Brecciation

The "Cooley Breccias" are tectonic breccias formed along the reverse faults within the steep to overturned, brittle dolomitic lithologies of Teena, Mitchell Yard and Mara Dolomite which were overthrust against and over Barney Creek Formation lithologies. The breccias commonly show a zonal arrangement of increasing deformation approaching reverse faults, from fracture networks without any disaggregation, through an angular fragmental zone with minor separation and rotation, through zones of increasing disaggregation and rotation and fragment rounding to zones of significant fragment disaggregation, random orientations and sometimes significant rounding (see Accompanying Section Legend). The reverse faults are commonly marked by an early broad zone of redolomitization / recrystalization sometimes containing silica (chalcedony) blebs (Mitchell Yard) which can contain small scale, pre-brecciation, folding (alteration-recrystallization softening).

The tectonic breccia matrix comprises finer grained (grit-sand-silt size) fragments of the brecciated dolomites that commonly show grading (geopetal) within individual interstices and light to medium to dark grey "shale". This "shale" comprises fine grained dolomite, and pyrite and probably is a sedimented chemical precipitate rather than a true matrix sediment (further work required). The darkest grey matrix material is commonly pyritic and sometimes pyritic-chalcopyritic.

In the footwall of the Basal Cooley Reverse Fault dolomitization, re-brecciation and copper(-lead) mineralisation occurs within the sedimentary breccias. Deformation probably focussed along shallowly to moderately NE dipping shaly horizons within the breccia pile resulting in re-brecciation, fluid flow and mineralisation in the surrounding breccias. The silty tops of breccia cycles are commonly dolomitized/recrystallised in the footwall of the Basal Cooley Reverse Fault and the "Cooley breccia" style (and generation) of copper mineralisation is most strongly developed within the sedimentary breccias of the Main Talus Breccia and Lower Pyritic Shale units.

Copper Paragenesis

A preliminary paragenesis of the copper mineralisation in the "Cooley Breccias" in the hangingwall of the Basal Cooley Reverse Fault based on core observations is presented in Figure 5.

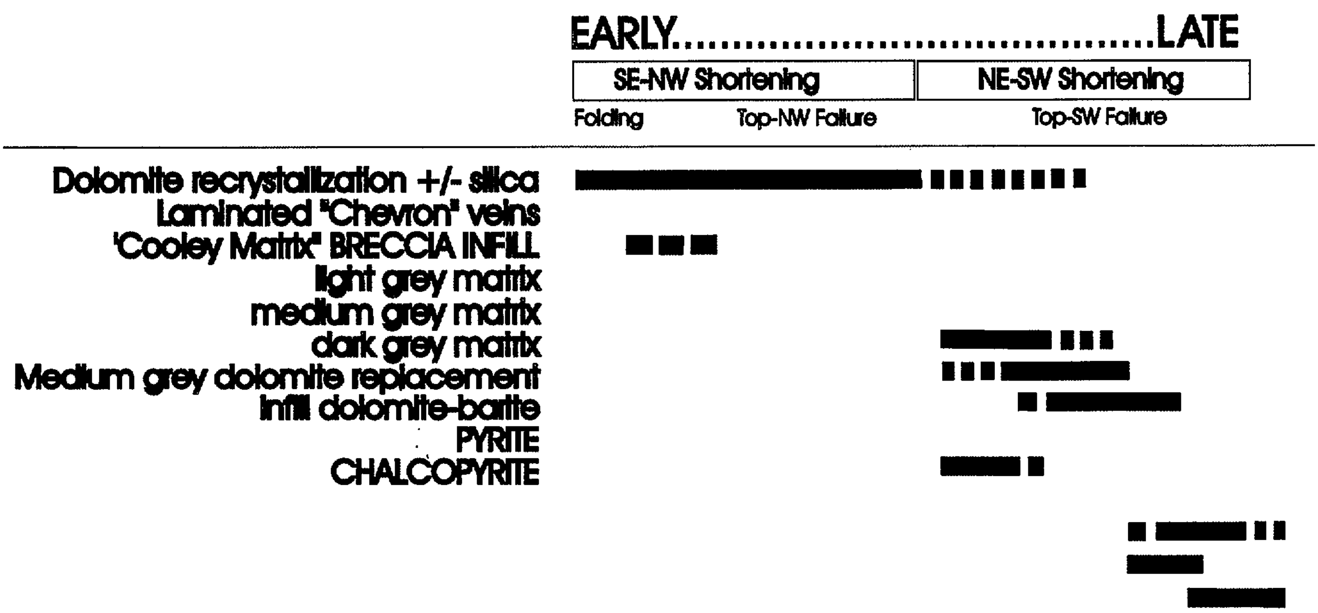

Figure 10. Paragenesis of the Cooley Breccia Copper Mineralization

This paragenesis has not been fully fixed relative to the structural-kinematic evolution of the Cooley Zone, however, some constraints incorporated into Figure 10 are known:

a) the dolomite recrystalization occurs along with the earliest phase of reverse fault failure (most probably NW transpressively directed)
b) The Chevron Veins are commonly at a high angle to bedding and suggest layer-parallel extension in the early stages of macroscopic folding
c) the terminal phase of pyrite±chalcopyrite mineralisation is synchronous with "Top-to-SW" kinematic failures. Copper mineralisation associated with extensional veins and ?clay/talc alteration on failed bedding is strongly associated with "Top-to-SW" kinematics on shallow dipping thrusts at the end of N28-99E in the footwall of the Basal Cooley Reverse Fault.

LATE FAULTING

Two late fault sets can be resolved within the drillcore data that are consistent with other mapped faulting at HYC-Cooley. The first set strike NE-SW and have reverse oblique-slip to strike-slip movements (F4 on Structural Overlay; Fig. 8). Faults of this generation include Woyzbun, McArthur River and possibly a reactivation phase of N33 (see Fig. 11). The second set have more NW-SE'ish trends with oblique-slip to strike-slip movements and are correlatives of the Cross Cut Fault from underground and the H20, I20 and I19 Faults from the structural drilling program.

BARNEY HILL-HYC-COOLEY STRUCTURE

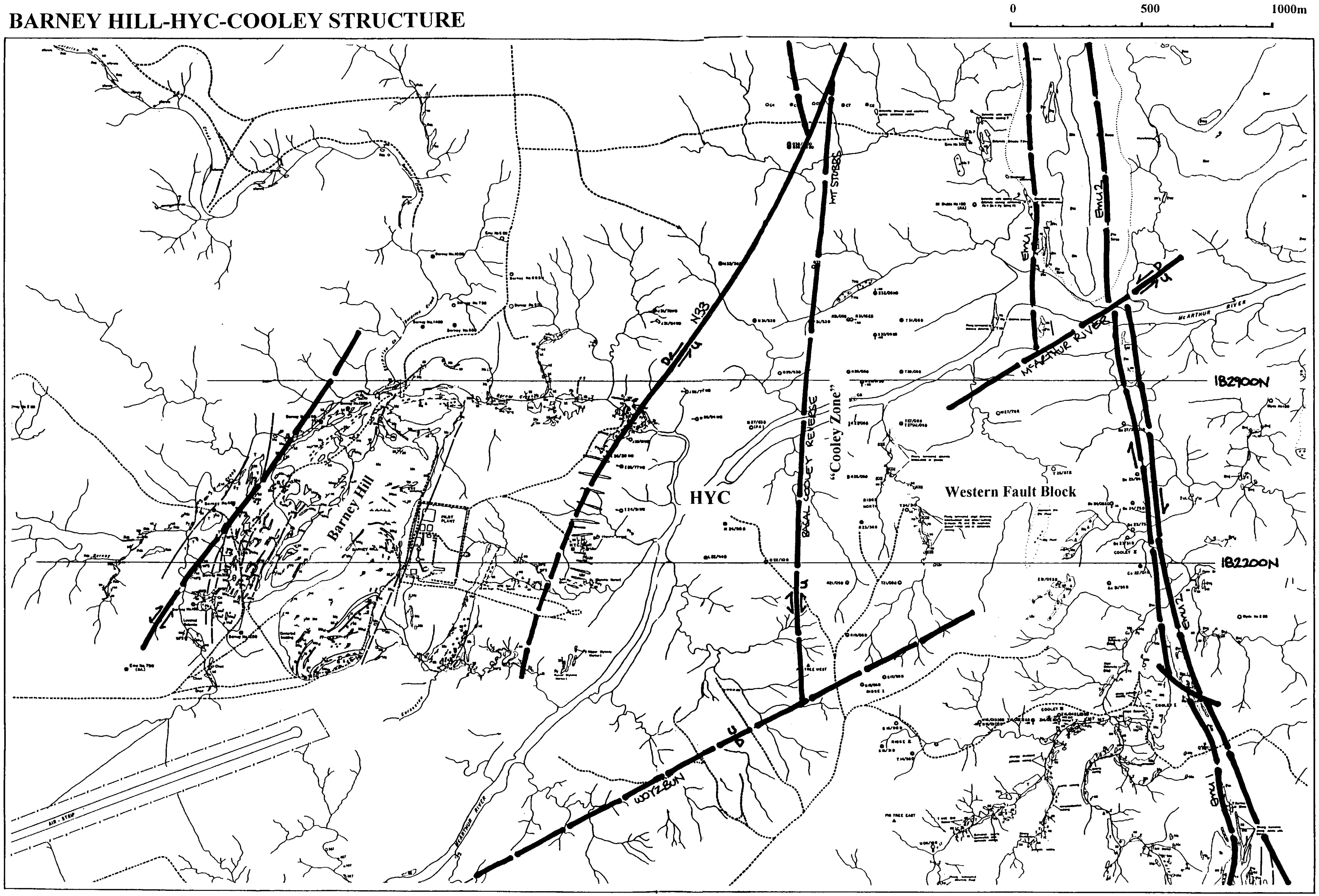

Compiled from MIMEX 1:5000 Geology by MCH, June, 1993

Figure 11.

SYNTHESIS and GEOLOGICAL HISTORY

Figure 12 illustrates in cartoon form the structural-kinematic evolution of the Barney Hill-HYC-Cooley-Emu section from the initiation of Barney Creek sedimentation, through the "Cooley" inversion to the regional major N-S shortening episode (probably correlative of Mt Isa D1) to produce the final geometry depicted in Figure 6. The extensional/shortening directions and kinematics indicated on the Figure are appropriate for the local HYC-Cooley domain and do not necessarily reflect regional stress orientations.

Barney Creek Sedimentation

A thick sequence (up to ?800m+) of W-Fold, Lower Dolomitic, Lower Pyritic with sedimentary breccias, Main Talus Breccia, Bituminous, Upper Pyritic and Upper Dolomitic Shales deposited in an Emu-parallel elongate trough. This trough's eastern edge was somewhere east of the present trace of the Emu Fault (5-10km east based on Emu-parallel magnetic structure) and its western edge lay approximately through the present Barney Hill (magnetic edge).

Within the trough (Emu Trough), sedimentary breccias of the Lower Pyritic Shale and Main Talus Breccia flowed, from an entry point north of HYC, to the south and southwest (Logan, 1979). The sedimentary breccias within the Barney Creek Formation record the progressive exhumation of the pre-Barney Creek dolomitic McArthur Group stratigraphy. This implies that the provinence region for the sedimentary breccias (somewhere adjacent and close to this Emu Trough) was being actively uplifted and eroded during Barney Creek-time. Tectonically this is not possible in a purely extensional regime: it seems likely that this Emu Trough zone was transpressive-transtensional throughout much of Barney Creek-time (Fig. 12) and that transpression ultimately inverted the HYC Emu Trough forming the Western Fault Block and the "Cooley Breccias".

The nature of the western margin of the Emu-parallel trough is unknown. It has not apparently reactivated during later deformations in the way the Emu Fault has, suggesting that this boundary of the trough may be a hinge line rather than a major fault or set of faults.

Subsidence within the HYC portion of the Emu Trough west of the present Emu Fault was most rapid in the NE. Breccias, which thin to the south and west in the HYC area, are envisaged to have filled the additional space created by the heterogeneous subsidence. As a result of this differential subsidence, buried sedimentation surfaces (bedding) within the diagenetically maturing pile adopted gentle and steepening NE dips. The zone was probably seismogenic which triggered failures on bedding producing the kinematically dominant "Top-to-NE" compressional and extensional structures (see below; Fig. 4). These structures post date a number of diagenetic features including crusts, concretions, biogenic pyrite and probably Pb-Zn mineralisation (Fig. 5) all of which formed at considerably shallower (some close to or at zero) depths of burial.

These observations are consistent with a deviation from the regional tectonic framework during Barney Creek-time (Etheridge & Wall, 1994) in which Emu parallel structures become transpressive-transtensional. Local transtension at HYC within the active Emu zone resulted in more rapid subsidence and the accumulation of the anomalously thick Barney Creek HYC sequence within the Emu Fault Trough. Transtension across the HYC basin bounding faults would have made them dilational and have aided base metal bearing hydrothermal fluid access.

Pre-Barney Creek (McArthur Group) time
N-S Extensional Geometry (Etheridge & Wall)
early syn-diagenetic dolomitization

Start of Barney Creek time
W-Fold Shale
Transpressive-Transtensional EMU ZONE

Lower HYC Pyritic Shale time
HYC Rapid Subsidence
Elsewhere uplift - NE sedimentary breccia source
Syn-diagenetic HYC Pb-Zn Mineralization

"Main Talus Breccia" time
NE Maximum Subsidence - TNE Bedding Failure
Warping - sedimentary breccia channelling

Upper Stylolitic Marker time ~1640Ma
NE Maximum Subsidence - TNE Bedding Failure
Folding - sedimentary breccia channelling

Upper Pyritic & Bituminous Shale time
NE Maximum Subsidence - TNE Bedding Failure
Overturned Short Limbs

Upper Breccia time
Short Limb Transpressive Failure - TNW Kinematics
Upper Breccias sourced from Western Fault Block
Cooley Brecciation - (re)dolomitization
(HYC North Cu-Pb Mineralization)

2nd Phase Transpressive Failure - TSW Kinematics
"Cooley Breccia" Cu-Pb Mineralization
in Western Fault Block & "Main Talus Breccia"

Upper Barney Creek ONLAP
Reward Dolomite Sedimentation
Batten Subgroup Sedimentation

Regional N-S Deformation (Isan D1 ~1600Ma)
Emu Fault Zone - DEXTRAL STRIKE SLIP
NE faults - oblique to strike slip
Vein MVT Cu-Pb Mineralization
Cooley Cu, Cooley Pb adjacent to EFZ

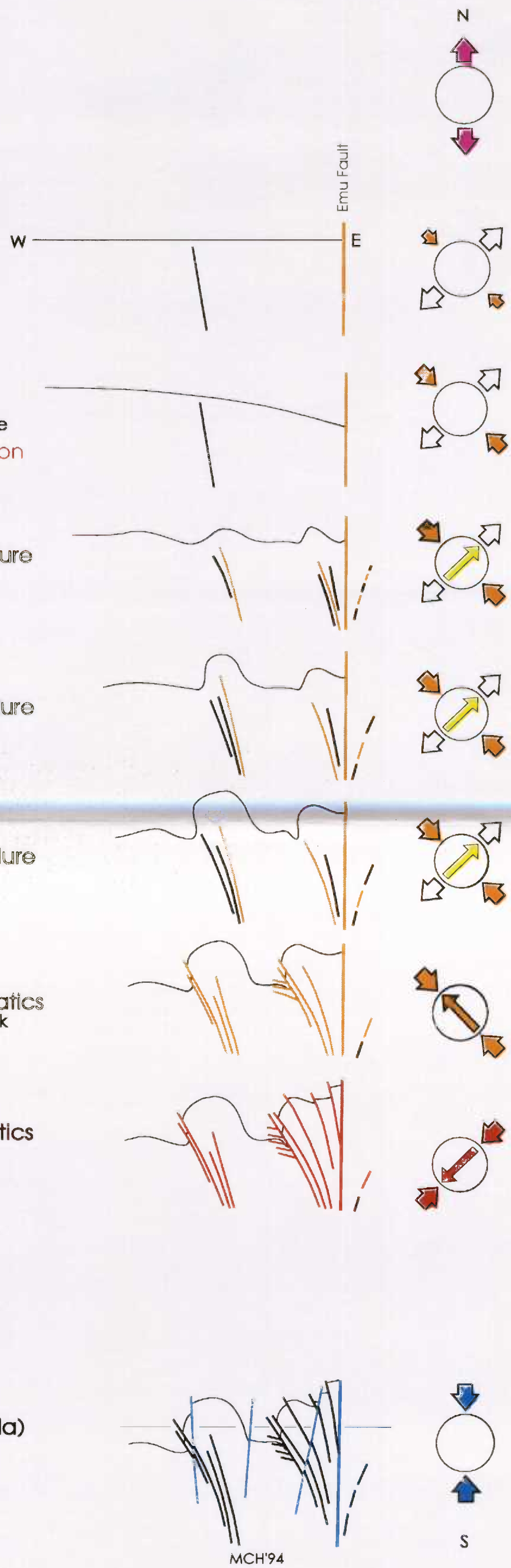

Figure 12. Structural-Kinematic Evolution of the Barney Hill - HYC-Cooley Section

Transpressive Inversion and Shortening

During continued deposition of the Barney Creek Formation, the HYC area began to invert. This transpressive inversion focussed (1) along the Emu Fault (reactivating it as a transpressive, positive flower structure), (2) along some NE-trending structure under Barney Hill and (3) possibly also along the western margin (?hinge line) of the Emu Trough. Shortening was approximately SE-NW directed and produced the NE trending Barney Hill Anticline and associated parasitic folds and more Emu-parallel folds closer to the Emu Fault (shear component of strain taken up along the Emu Fault resulting in local shortening being more normal to the structure). A crude cleavage nucleated in shaly units closer to the Emu Fault where shortening was more intense. The folds in the Lower HYC sequence and underlying dolomitic stratigraphy at Barney Hill and at Cooley progressively tightened, while Barney Creek sedimentation continued at the sediment-water interface above, until they developed overturned west limbs which subsequently failed.

"Top-to-NW" and "Top-to-SW" Failure

Ultimately the western short limbs fail. The gross geometry of the major structures is not sufficiently clear to resolve whether the shallow thrust failures, which are mostly "Top-to-NW" kinematically, pre-date or are synchronous with the steeper reverse transpressive faults of the overthrust "Cooley Zone". What is clear is that there are two kinematic phases within the shallow footwall thrusts with the "Top-to-NW" preceding "Top-to-SW" kinematics and well developed "Top-to-SW" kinematics in the steeper reverse faults within the "Cooley Zone". Dolomitization and recrystallization along the major reverse faults and thrusts is associated with the earlier phase of failure while copper mineralisation appears to be linked with the "Top-to-SW" phase of movement in the footwall zone (more detailed oriented core work required within hangingwall "Cooley Zone").

In a regional tectonic sense it is unclear what controls this rotation of the local shortening direction and kinematic transport direction, however, it can be rationalised in terms of the interaction of regional scale structures (Etheridge & Wall, 1993; unpubl. company report) The NE-SW phase of shortening could result from an initial pulse of NS shortening modified locally at HYC by synchronous right lateral reactivation of the Emu Fault. This shortening phase most probably produces the opposite-sense, "Top-to-SW" low angle structures within the HYC ore sequence (Fig. 4).

Upper Breccia sedimentation is hypothesised to be linked with these transpressive failure phases. The formation of a positive flower structure along the reactivated Emu Fault would provide a more local source (Logan, 1979) for the Teena to Masterton lithologies present within the Upper Breccias deposited west of the "Cooley Zone".

R9500517

Figure 13. The Sedimentary Architecture at McArthur River

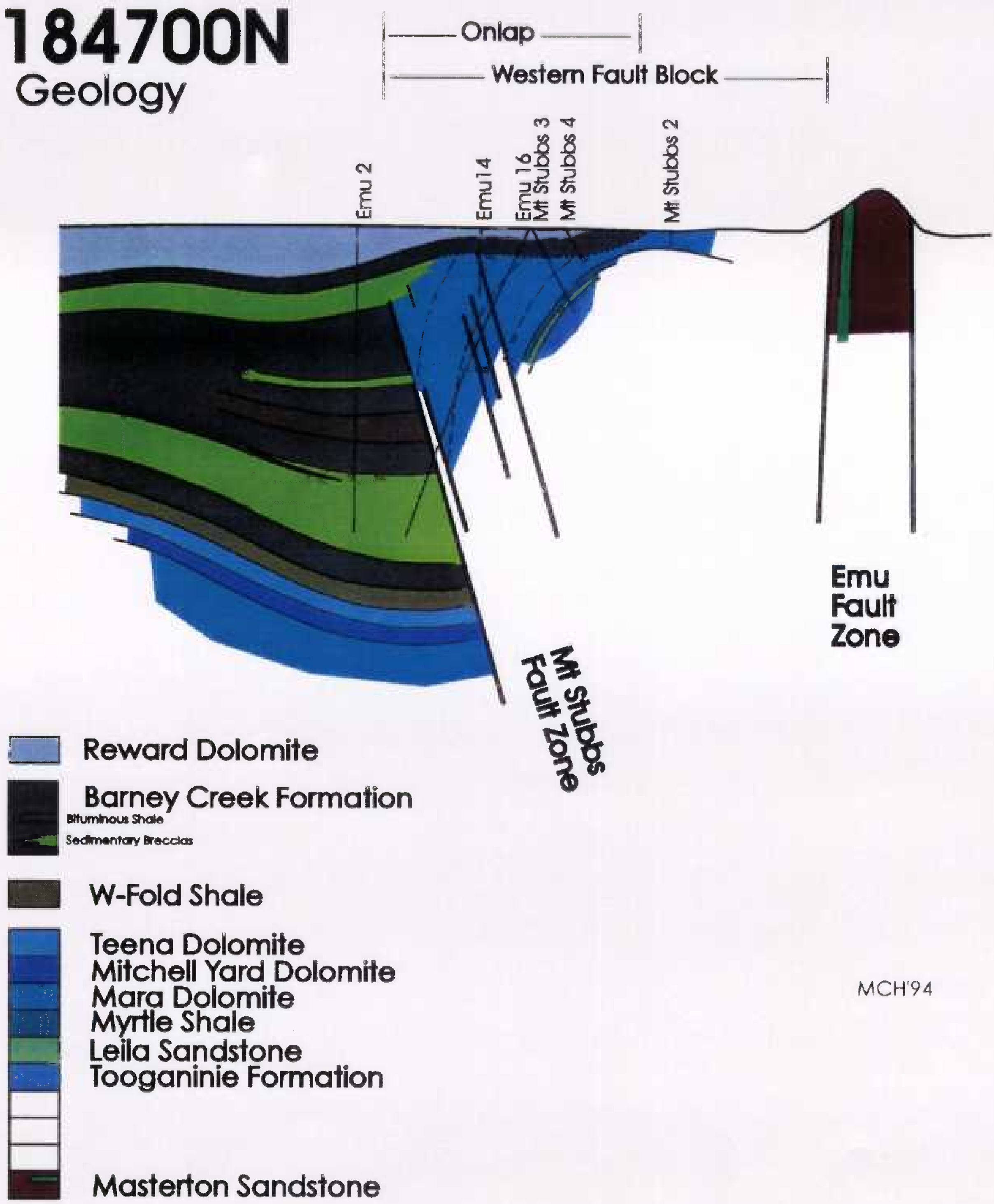

Figure 14. Section 184700N Geology

Figure 15. Schematic Onlap Geometries

Upper Barney Creek Onlap, Reward Dolomite and Batten Subgroup Sedimentation

As the transpressive deformation quietened, Upper Breccia sedimentation passed into Upper Barney Creek sedimentation at HYC. West of HYC breccias are not present and HYC shale sedimentation passes conformably into Reward Dolomite sedimentation. North of HYC, condensed? (atypical) Upper Barney Creek sediments were deposited with a high angle unconformity over the steeply-dipping, upthrust, redolomitized and mineralised Mara Dolomite lithologies of the “Cooley Zone” or Western Fault Block (Fig. 14). Present drilling geometries indicate that north of HYC, Cooley transpression-generation structures do not cut Upper Barney Creek and Reward Dolomite sedimentation (locally later structures and reactivations may do so; Fig. 14).

It is suggested that onlap onto the "Cooley Zone" may have developed in other localities *during* Upper Breccia deposition if the westernmost reverse fault became inactive while reverse structures further east continued to be transpressively active (Fig. 15). The relationships at Ridge, where strataform, shale-hosted Pb-Zn mineralisation at the base of the Upper Breccias ?unconformably overlies Cooley-brecciated and mineralised (probable) Teena Dolomite suggest this (Fig. 15).

Reward Dolomite and the Batten Subgroup was deposited over the Barney Creek Formation with transitional conformable relationships around McArthur-HYC. These unit probably completely overlapped the "Cooley Zone", Western Fault Block and Emu Fault Zone which was inactive at this time.

North-South Shortening ca.1600Ma

North-south (or probably more NNE-SSW) shortening folded the Reward and Batten Subgroup units and reactivated the Emu Fault as a right lateral strike-slip structure cutting these units probably during the regional Isan D1 deformation. Prominent east-west to WNW-ESE fold axes northwest of HYC (Figs 1 & 13) reflect this deformation. Closer to the Emu Fault more Emu-parallel folds formed due to the local strike-slip shear release along the Emu Fault. North-south thrusting also occurred locally on shallowly dipping contacts between units (north of HYC; Figs 1 & 13).

The Cooley Lead mineralisation immediately adjacent to the Emu Fault lies along a shallowly dipping, brecciated contact between Mara and Tooganinie and steeply north-dipping dilational veins in Mara above the brecciated zone. Bedding offsets across the veins are consistent with North-Block-Down and suggest "Top-to-South" movement of Mara over Tooganinie adjacent to the Emu Fault. This mineralisation and probably also Cooley Copper are therefore timed to be synchronous with the right-lateral reactivation of the Emu Fault during the regional (Isan D1) NS shortening event (ca. 1600Ma).

During this NS shortening at HYC-Cooley(-Emu) NE-trending faults showing oblique reverse to strike-slip movements (Woyzbun, N33 reactivation and McArthur River Faults; Figs 1 & 11) formed or reactivated. Some faults of this generation cut the Emu Fault (eg. McArthur River Fault).

REFERENCES

Etheridge, M. & Wall, V., 1994. Tectonic and structural evolution of the Australian Proterozoic. *Geological Society of Australia, Abstracts No.* **37**, 12th AGC, Perth

Hinman, M.C., 1993. A Lotus 1-2-3 diamond drillhole structural manipulation spreadsheet: Drillcore structural data generation. *Computers & Geosciences* **19**, No. 3, 343-354

Logan, R.G., 1979. The geology and mineralogical zoning of the HYC Ag-Pb-Zn deposit, McArthur River, NT, Australia. *Unpubl. Msc Thesis*, Australian National University

APPENDIX

Drillhole Structural Logs of N28-99E, I22-55, K22-55 and R29-05.

HOLE	SURVEY DATA Dpth	SURVEY DATA Plng	SURVEY DATA Dir	DPTH	PLNG	DIR	d	DipAzm or C/Oa	LOCAL S0 Dip	LOCAL S0 Dir	?	d	(C/O) a	Sa Dip	Sa Dir	?	d	(C/O) a	Sb Dip	Sb Dir	?	d	(C/O) a	Sc Dip	Sc Dir	?	B	La Plng	La Dir	90 S0 Dip	90 S0 Dir	90 Sa Dip	90 Sa Dir	90 Sb Dip	90 Sb Dir	90 Sc Dip	90 Sc Dir
N28/99	30.0	63.0	96.0																																		
				32.5	63.0	96.0	27	165	7	359	Emf	52	-48	72	238															0	270	69	270				
				32.7	63.0	96.0	27	175	2	4																				0	90						
				32.8	63.0	96.0	43	10	33	10	V	54	180	73	234															6	90	69	270				
				41.7	63.0	95.8	30	10	12	10	Emf	50	140	65	227															2	90	58	270				
				43.2	63.0	95.8	23	40	9	220	Fault	23	0	9	220											T-FA	90	9	204	6	270	6	270				
				46.5	63.0	95.7	29	10	9	10	Emf	60	145	78	230															2	90	74	270				
				50.0	63.0	95.7	30	10	11	10	Emf	48	150	67	235															2	90	62	270				
	60.0	63.0	95.5																																		
				61.5	62.7	95.3	30	10	11	10	Emf	50	145	68	232															2	90	63	270				
				62.3	61.0	94.5	30	150	15	355																				1	270						
				62.5	63.1	95.5	30	150	14	4																				1	90						
				62.7	63.1	95.5	35	155	15	26																				7	90						
				64.5	63.1	95.5	30	10	11	10	F&Vn	67	140	81	219															2	90	75	270				
				65.4	63.2	95.6	33	10	18	10	Emf	62	145	74	217															3	90	64	270				
				67.5	63.3	95.6	32	10	16	10	Emf	32	155	51	241															3	90	48	270				
				72.2	63.4	95.7	32	10	16	10																				3	90						
				73.8	63.5	95.7	31	10	15	10	mf	73	180	84	68											Slds	-35	13	36	3	90	83	90				
				76.5	63.6	95.8	33	10	18	10	mf	24	165	45	250	F	72	155	86	220										3	90	44	270	84	270		
				81.7	63.7	95.9	34	10	20	10	Emf	47	160	64	232															4	90	58	270				
				89.1	64.0	96.0	32	10	17	10	Emf	61	160	78	229											T-FA	80	12	325	3	90	74	270				
				89.1	64.0	96.0	32	10	17	10																Slds	50	5	295								
	90.0	64.0	96.0																																		
				91.1	64.0	96.0	31	10	16	10	FAULT	63	125	67	202															3	90	42	270				
				94.8	64.0	96.0	33	10	19	10	Ef	66	155	80	221															4	90	75	270				
				96.7	64.0	96.0	31	10	16	10	Faults	63	110	61	189	mf	57	160	75	233						fSlds	-60	0	99	3	90	15	270	71	270		
				98.6	64.0	96.0	31	10	16	10	Emf	32	150	49	238	F&Vn	50	150	65	228										3	90	45	270	58	270		
				103.0	64.0	96.0	28	10	9	10	Ef	60	150	78	234															2	90	76	270				
	105.0	64.0	96.0																																		
				113.0	64.2	96.0	28	10	9	10	Ef	44	150	63	239											Slds	30	1	288	2	90	59	270				
				119.0	64.3	96.0	27	10	7	10	Ef	53	155	74	244															1	90	72	270				
				122.0	64.4	96.0	26	160	9	360																				0	270						
				122.5	64.4	96.0	30	145	17	5																				2	90						
				123.0	64.4	96.0	30	155	12	15																				3	90						
	126.0	64.5	96.0																																		
				131.3	64.5	95.8	28	40	5	41	Ef	58	145	78	240											Slds	-45	4	44	3	90	76	270				
				134.0	64.5	95.7	27	45	2	46	mf	62	150	84	246	T	15	10	11	267	Ef	35	10	10	117					2	90	83	270	11	270	9	90
	138.0	64.5	95.5																																		
				139.1	64.5	95.5	25	90	0	269	V	86	-140	75	137															0	270	68	90				
				146.2	64.8	95.8	26	100	1	100	V	83	85	82	184															1	90	27	270				
				148.5	64.9	95.9	25	110	0	296	Ef	30	15	8	157	V/2	75	75	70	179										0	270	3	90	4	90		
				151.6	65.0	96.0	26	110	1	109																Slds	20	1	116	1	90						
	152.0	65.0	96.0																																		
				152.5	65.0	96.0	27	120	2	119	Emf	56	120	71	228															2	90	65	270				
				152.8	65.0	96.0	34	120	10	120	V/2	74	90	78	199															8	90	58	270				
				155.0	65.0	96.0	34	-170	10	129																				8	90						
				155.5	65.0	96.0	35	-175	10	112																				10	90						
				156.2	65.0	96.0	28	-175	4	135																				3	90						
				158.0	65.0	96.0	42	120	18	120	sgV	62	140	84	250															16	90	84	270				
				161.5	65.0	96.0	35	120	11	120	Ef	67	150	90	75															9	90	90	90				
	162.0	65.0	96.0																																		
				163.1	65.0	96.0	33	120	9	120	Ef	60	150	83	256															7	90	83	270				
				168.8	65.2	96.2	30	120	6	120	Ef	70	140	89	63															5	90	89	90				
				171.3	65.3	96.3	36	120	12	120	Emf	60	147	83	255	cEV	65	125	83	235										10	90	82	270	81	270		
	177.0	65.5	96.5																																		
				178.1	65.6	96.5	33	120	9	120	cEV	75	140	84	64															8	90	84	90				
				178.7	65.6	96.6	35	120	11	120	Emf	30	135	51	254	cEV	56	140	77	250										10	90	50	270	77	270		
				180.8	65.7	96.6	30	120	6	120	cEV	57	140	78	247															5	90	77	270				
				184.3	65.9	96.7	36	120	13	120	cEV	63	140	84	249															11	90	84	270				
				187.4	66.1	96.8	42	120	19	120	mf	45	140	67	255	cEV	60	140	81	252										17	90	66	270	81	270		
				189.0	66.1	96.9	33	120	10	120	V	66	120	81	229															8	90	79	270				
				190.5	66.2	97.0	50	120	27	120	cV	70	155	87	86															24	90	87	90				
				191.7	66.3	97.0	42	120	19	120	cEV	55	147	77	259	sgV&F	67	-165	89	301						fSlds	90	4	197	17	90	77	270	88	270		
	192.0	66.3	97.0																																		
				193.3	66.3	97.1	33	120	10	120	Ef1	53	135	73	246	sgV2	70	-155	90	127										9	90	71	270	90	90		
				195.5	66.4	97.2	27	120	4	120																				3	90						
	200.0	66.5	97.5																																		
				201.1	66.4	97.6	37	120	14	120	T1	40	0	17	117	cEV1	58	125	75	238	mf2	58	125	75	238					12	90	15	90	73	270	73	270
				201.8	66.4	97.6	48	120	25	120	cEV	55	155	78	267	F	47	170	71	280										22	90	78	270	70	270		
	227.0	65.0	99.0																																		
	239.0	65.0	93.0																																		
	251.0	65.0	92.0																																		
	263.0	65.0	92.5																																		

				263.0	65.0	92.5					cstS0	48																								
	272.0	65.0	88.5																																	
				278.0	64.5	88.0					cstS0	85																								
				282.0	64.2	87.7	60	40	40	40																				28	90					
				282.5	64.1	87.6	68	40	49	40	StylF	78	-10	61	33															36	90	45	90			
				283.4	64.1	87.6	85	255	70	75	Fault	85	0	70	75											Slds	-75	9	162	69	90					
	284.0	64.0	87.5																																	
				287.0	64.0	87.4	40	40	18	40																				12	90					
				287.6	64.0	87.4	34	40	11	40																				7	90					
				290.5	64.0	87.3	50	40	29	40																				20	90					
				295.0	64.0	87.2																														
				297.8	64.0	87.1	67	40	47	40																				35	90					
				298.8	64.0	87.1	30	40	5	40																				4	90					
				299.0	64.0	87.1	50	40	29	40																				20	90					
				299.5	64.0	87.1	55	40	34	40																				24	90					
				300.4	64.0	87.1	35	165	12	40																				8	90					
				301.0	64.0	87.1	45	40	23	40																				16	90					
	303.0	64.0	87.0																																	
				313.1	64.0	86.2					Styl	65	-65	88	292																	88	270			
N28-99b	321.0	64.0	85.5																																	
				328.0	64.0	85.4	70	175	44	79	mf	40	0	66	265															44	90	66	270			
				329.0	64.0	85.4	88	0	66	85	f	60	180	34	85															66	90	34	90			
				330.0	64.0	85.4	80	10	74	96																				74	90					
				334.0	64.0	85.4	45	20	70	280	f	52	-105	50	182															70	270	2	270			
				335.5	64.0	85.3	25	-90	44	206	f	42	45	63	298	sgV	80	90	81	351										23	270	60	270	45	270	
				336.5	64.0	85.3	22	75	38	302	S1	85	170	59	74															33	270	58	90			
				336.7	64.0	85.3	18	80	34	299	S1/mf	80	175	54	79															30	270	54	90			
	339.0	64.0	85.3																																	
	347.0	61.5	87.0																																	
				348.2	61.5	87.0	35	-70	51	223	f/sgV	80	45	80	132															40	270	76	90			
				349.0	61.5	86.9	32	-85	44	217	S1/mf	85	160	58	63															30	270	56	90			
				350.2	61.5	86.9	27	-65	46	232	S1/mf	80	140	59	39	f2	68	105	64	359										40	270	47	90	2	270	
				351.0	61.5	86.8	28	-100	35	214																				22	270					
				351.5	61.5	86.8	47	-140	30	157																				13	90					
				353.0	61.5	86.8	25	-110	30	214																				18	270					
				354.0	61.5	86.7	33	-125	28	192	f2	53	35	77	295															6	270	76	270			
				354.3	61.5	86.7	35	-140	22	177	f1	53	0	82	267															1	90	81	270			
				354.5	61.5	86.7	50	-165	23	117																				21	90					
				354.6	61.5	86.7	70	-25	84	63	F	47	-50	68	230															83	90	62	270			
				354.8	61.5	86.7	50	-45	72	232																				68	270					
				355.5	61.5	86.6	28	-90	39	218	sgV	58	15	86	279															27	270	86	270			
				356.4	61.5	86.6	48	-65	64	218	sgV	73	180	45	87	f3	45	75	58	320										52	270	44	90	45	270	
				357.5	61.5	86.6	55	-90	68	189																				22	270					
				358.0	61.5	86.5	47	-85	55	204	fs	30	65	49	304															31	270	43	270			
				358.2	61.5	86.5	43	115	39	348																				10	270					
				358.5	61.5	86.5	62	-105	59	178																				3	90					
				359.0	61.5	86.5	35	115	33	338	sgV	83	120	70	20															14	270	43	90			
	359.0	61.5	86.5																																	
				362.2	61.6	86.3	30	175	3	27																				1	90					
				364.9	61.6	86.1	43	160	19	39	F	40	160	16	33															12	90	9	90			
				364.9	61.6	86.1	47	125	37	0																				0	90					
				365.1	61.6	86.1	52	110	48	352	f1	67	-40	90	230	f2	45	179	17	84										9	270	89	270	17	90	
				365.5	61.6	86.1	48	115	42	353	f	75	-70	86	201															7	270	79	270			
				367.8	61.6	85.9	44	125	35	357																ITF	75	16	291	2	270					
				368.6	61.7	85.9	43	155	20	30	f	75	-100	72	174															11	90	17	90			
				369.4	61.7	85.8	48	-140	31	155	f1	75	130	59	26	sgV	72	-100	69	176										14	90	35	90	11	90	
				371.2	61.7	85.7	42	-170	15	113	sgV	75	70	86	331															14	90	82	270			
				375.1	61.8	85.5	50	155	27	39	mf	47	-30	72	243															17	90	70	270			
				375.6	61.8	85.4	55	140	37	24	fs	65	-145	44	134															17	90	34	90			
				376.5	61.8	85.4	50	150	28	32	f	75	0	77	85															16	90	77	90			
				379.2	61.8	85.2	43	150	23	22	f1	45	-50	66	229	sgV2	56	70	69	322										9	90	59	270	58	270	
				382.5	61.9	85.0	60	140	41	27																ssFA	-55	36	352	22	90					
	390.0	62.0	84.5																																	
				404.3	62.0	84.7	55	120	46	2																				2	90					
				404.5	62.0	84.7																														
				405.5	62.0	84.8	65	65	79	322																				72	270					
				405.9	62.0	84.8	65	150	42	42	mf	60	145	39	33															31	90	24	90			
				407.0	62.0	84.8	63	140	44	29	S1	63	140	44	29	mf2	65	0	87	85	f3	23	40	48	285					25	90	25	90	87	90	47
				407.3	62.0	84.8	42	140	26	8	S1	75	-55	88	32															4	90	87	90			
				408.3	62.0	84.8	53	100	53	343																				21	270					
				409.9	62.0	84.8	65	160	39	56	f/V	75	-30	81	56															34	90	79	90			
				412.6	62.0	84.9	57	-175	29	93																				29	90					
				413.0	62.0	84.9	44	150	23	24	mf	20	-30	46	251															10	90	45	270			
				414.0	62.0	84.9	60	145	39	33	T	35	150	17	6	f	50	-40	73	234										24	90	2	90	69	270	
				415.2	62.0	84.9	55	120	46	2	Ts	40	135	27	0															2	90	0	90			
				415.4	62.0	84.9	57	150	35	38																				23	90					
				416.8	62.0	84.9	65	175	37	77																				36	90					
				418.5	62.0	85.0	88	0	64	85	f	20	-15	48	258															64	90	47	270			

			420.0	62.0	85.0	88	-20	66	63															63	90				
420.0	62.0	85.0																											
			421.0	62.0	85.0	85	-180	57	85															57	90				
			422.0	62.0	85.0	70	20	84	104															83	90				
			422.5	62.0	85.0	65	170	38	70	DC	20	180	8	265										36	90	8	270		
			423.0	62.0	85.0	60	70	72	324	fs	45	10	73	272										62	270	73	270		
			423.2	62.0	85.0	63	20	90	283	f	90	0	62	85										90	270	62	90		
			423.5	62.0	85.0	47	15	74	276															74	270				
			424.5	62.0	85.0	42	115	38	346															11	270				
			425.4	62.0	85.0	67	0	85	85											Slds	75	15	-4	85	90				
			426.0	62.0	85.0	30	50	52	294															50	270				
			428.0	62.0	85.0	52	60	69	312															63	270				
			430.3	62.0	85.0	75	25	79	110															79	90				
			432.6	62.0	85.0	63	30·	88	291															88	270				
			435.0	62.0	85.0	62	45	83	304															82	270				
			436.5	62.0	85.0	75	50	86	133	Tf	40	-140	25	165										85	90	7	90		
			438.0	62.0	85.0	70	80	77	337	Tf	57	-125	45	161										60	270	18	90		
			438.4	62.0	85.0	65	65	79	322	T	52	-140	34	149										72	270	19	90		
			439.8	62.0	85.0	75	40	83	124	T	45	-130	33	168										82	90	8	90		
			441.0	62.0	85.0	60	35	84	295	T	57	-160	32	118	f	35	-60	54	227					83	270	29	90	45	270
			443.6	62.0	85.0	60	55	78	311	f	13	-80	33	241										74	270	29	270		
			443.7	62.0	85.0	55	50	75	306	T	30	80	44	311	f	68	35	89	117					72	270	36	270	88	90
			444.7	62.0	85.0	60	55	78	311	F	48	25	74	284										74	270	74	270		
			445.0	62.0	85.0	52	45	74	301	Fs	40	-150	20	153						FSlds	55	20	166	71	270	10	90		
			445.7	62.0	85.0	50	35	74	292	Fs	53	35	77	293						FA	-50	53	224	73	270	76	270		
			447.0	62.0	85.0	85	75	87	159	S/mf1	40	100	43	333	F2	38	-10	66	258					83	90	23	270	65	270
			448.0	62.0	85.0	43	140	27	10															5	90				
			449.0	62.0	85.0	40	135	27	0															0	90				
			449.5	62.0	85.0	40	145	23	11	F3	85	-35	72	48						FSlds	-25	46	119	5	90	67	90		
			450.0	62.0	85.0	47	-110	44	183	F2	55	-50	75	224						FSlds	-6	59	161	3	270	69	270		
450.0	62.0	85.0																											
			450.6	62.0	85.0	50	-160	25	123	S1	70	-115	61	162	F	43	0	71	265					21	90	28	90	71	270
			451.4	62.0	85.0	55	160	30	51															24	90				
			451.6	62.0	85.0	65	55	83	313															80	270				
			452.0	62.0	85.0	58	165	32	60															28	90				
			452.1	62.0	85.0										FAULT	35	155	35	196									11	270
			452.5	62.0	85.0	65	85	70	338															46	270				
			453.5	62.0	85.0	65	85	70	338	F	25	-70	43	229	F	23	90	45	323					46	270	35	270	31	270
			454.0	62.0	85.0	40	115	36	343	S1	75	-90	77	182	FAULT	40	0	68	265					12	270	9	270	68	270
			454.5	62.0	85.0	53	-110	49	178															2	90				
			455.2	62.0	85.0	58	-135	41	150	Fs	44	45	66	297										24	90	63	270		
			456.5	62.0	85.0	52	-115	46	175	F	72	80	79	338						FSlds	65	3	248	5	90	62	270		
			457.6	62.0	85.0	55	-105	53	181	F/V	52	15	79	277										1	270	79	270		
			458.6	62.0	85.0	40	-100	43	197	f	37	45	60	295										16	270	57	270		
			459.4	62.0	85.0	25	155	11	329															6	270				
			459.8	62.0	85.0	30	140	19	343															6	270				
			460.4	62.0	85.0					FAULT	55	-85	83	273												83	270		
			460.5	62.0	85.0	70	-85	75	189															30	270				
			461.5	62.0	85.0	70	-75	79	197															57	270				
462.0	62.0	85.0																											
452.0	60.0	87.0																											
456.0	59.3	87.0																											
464.0	56.3	87.5																											
			465.8	56.3	87.3	50	70	67	319															57	270				
			466.5	56.3	87.3	58	75	71	327	fs	34	-100	42	212										58	270	25	270		
			467.3	56.3	87.2	80	65	85	151															80	90				
			467.5	56.4	87.2					FA/Flt	63	-90	69	192										0	90	28	270		
			467.5	56.4	87.2	35	-95	45	213															28	270				
			468.0	56.4	87.1	30	-90	49	212															32	270				
			469.0	56.4	87.1	50	-110	47	188															8	270				
			469.8	56.4	87.0	65	-140	43	146	fs	47	110	45	343										27	90	16	270		
			470.5	56.4	86.9	60	95	63	343															30	270				
			470.8	56.4	86.9	90	-100	84	169															64	90				
			471.5	56.4	86.8	60	-125	46	166															14	90				
			472.5	56.4	86.7	60	-125	46	166															14	90				
			473.5	56.4	86.7	88	-80	86	6	F	30	-110	35	212	f2	35	0	69	267					58	90	21	270	69	270
			474.0	56.4	86.6	80	60	83	146	f	42	90	48	321	f	55	90	77	348					77	90	36	270	42	270
			476.0	56.5	86.4	67	-105	63	178	f	32	-80	49	223										5	90	38	270		
			477.5	56.5	86.3	67	110	60	359	f	35	50	61	296						fSlds	75	12	213	1	270	59	270		
			477.7	56.5	86.3	63	-140	41	147															25	90				
			478.8	56.5	86.2	80	-155	50	119															47	90				
			478.9	56.5	86.2	67	-155	38	125															33	90				
			482.2	56.6	85.9	67	-115	57	168	f	40	-45	67	236										17	90	63	270		
			481.5	56.6	85.9	62	-150	36	135	f2	20	-15	53	260										27	90	53	270		
			481.7	56.6	85.9	88	-130	67	142	cEV	40	-45	67	236										56	90	63	270		
			482.3	56.6	85.9	70	-150	43	130	cEV	40	-45	67	236										35	90	63	270		
			482.7	56.6	85.8					f2	55	0	88	266						fSlds	50	40	355	0	90	88	270		
			482.5	56.6	85.8					FAULT	35	80	51	312						FSlds	50	3	225	0	90	42	270		

				482.6	56.6	85.8	55	80	66	328	f2	12	-80	37	246	f2	15	-130	26	239										51	270	35	270	23	270		
				484.0	56.6	85.7	75	70	88	331																				86	270						
				486.0	56.6	85.5	67	65	84	323																				79	270						
				487.5	56.6	85.4	67	60	86	318																				84	270						
				489.0	56.7	85.3	67	60	86	318	F/V	45	-115	41	188															84	270	6	270				
				490.3	56.7	85.2	67	55	88	314	Stylbx	70	-65	86	207															87	270	81	270				
				491.8	56.7	85.0	47	70	64	315																				56	270						
	492.0	56.7	85.0																																		
				496.0	56.7	85.1	60	60	80	315																				76	270						
				497.5	56.7	85.1	60	60	80	315																				76	270						
				498.0	56.7	85.1	64	60	83	317																				80	270						
				500.2	56.7	85.1	60	60	80	315																				76	270						
				502.0	56.7	85.2	55	65	73	316																				66	270						
				505.0	56.7	85.2	65	65	82	321																				77	270						
				511.8	56.7	85.3					F	50	-65	80	288											fSlds	-45	60	215			80	270				
				516.2	56.7	85.4	67	70	81	326																				74	270						
				518.9	56.7	85.4	32	20	64	277																				64	270						
				521.6	56.7	85.5	55	30	85	290																				85	270						
				521.9	56.7	85.5	55	35	84	294																				83	270						
	522.0	56.7	85.5																																		
				523.0	56.7	85.5	67	60	86	319	f	22	-140	21	224	f	22	-140	21	224										84	270	15	270	15	270		
				524.5	56.7	85.5	45	70	63	314	f1	25	-90	43	221	f2	65	-70	79	205										54	270	31	270	67	270		
				525.5	56.7	85.5	46	100	50	334																				27	270						
				527.0	56.8	85.5	48	85	58	326	f	60	-40	87	232															42	270	86	270				
				528.0	56.8	85.6	43	80	57	319																				45	270						
				531.0	56.8	85.6	55	95	59	338																				31	270						
				531.8	56.8	85.6	45	75	61	317																				50	270						
				533.2	56.8	85.6	55	85	64	331																Slds	-50	61	304	45	270						
				534.6	56.8	85.6	50	135	33	6	pbV	25	-105	35	220															4	90	24	270				
				535.7	56.8	85.6	57	125	44	4																				4	90						
				536.9	56.8	85.6	55	120	45	358																				2	270						
				538.0	56.9	85.6	70	130	52	20																				23	90						
				539.0	56.9	85.6	68	135	48	23																Slds	90	23	316	24	90						
				541.0	56.9	85.7	78	155	49	52																Slds	85	10	331	42	90						
				542.7	56.9	85.7					F	30	-30	53	300											Fslds	70	14	222			49	270				
				544.4	56.9	85.7					1f	75	55	48	44											fSlds	-57	37	-2			38	90				
				545.8	56.9	85.7					1f	55	45	35	17											fSlds	70	10	302			12	90				
				546.3	56.9	85.7					1f	70	80	37	77											fSlds	15	35	102			36	90				
				562.5	57.1	85.8					C?HF	50	-55	77	296																	76	270				
				563.4	57.1	85.8					altfr	30	-155	53	233	altfr	25	-190	38	223	altfr	45	-165	62	217							47	270	28	270	48	270
				565.5	57.1	85.9	85	165	53	67	qcV1	20	90	38	300	qcV2	70	-90	75	186										51	90	34	270	21	270		
				566.2	57.1	85.9	75	135	54	28																SOSlds	-15	52	50	33	90						
				567.5	57.2	85.9	62	115	53	0	qcV	35	-80	51	219	qcV	25	-30	56	251										0	90	37	270	54	270		
				568.0	57.2	85.9	73	160	43	57	qcV/F	35	-85	49	216															38	90	34	270				
				569.6	57.2	85.9	75	165	44	65																				41	90						
				571.0	57.2	85.9	63	165	32	60	f	25	-155	14	219											fSlds	-15	8	274	28	90	9	270				
				572.0	57.2	85.9	78	165	47	66																				44	90						
				574.0	57.2	85.9					qcV	65	-120	85	62	qcV	45	-60	74	290												84	90	73	270		
				574.6	57.2	85.9	40	145	22	0	F	60	-50	83	224											FSlds	-70	5	313	0	90	80	270				
				576.2	57.2	86.0					Fs/qcV	40	-40	64	301											FSlds	80	17	220	0	90	60	270				
				576.2	57.2	86.0					Fs/qcV	40	-40	64	301											FSlds	-60	50	248			60	270				
				576.5	57.2	86.0	48	125	37	356																				3	270						
				578.5	57.3	86.0	57	155	30	40																				20	90						
				581.0	57.3	86.0	72	155	43	50	f	35	-20	67	254															36	90	66	270				
	582.0	57.3	86.0																																		
				583.5	57.3	86.0	75	150	48	45	f	25	65	48	297	f	30	-10	62	260						SOSld	-70	29	346	38	90	45	270	62	270		
				584.7	57.3	85.9	60	130	44	13	F	60	-10	88	77											FSlds	-50	35	166	12	90	88	90				
				585.9	57.3	85.9	85	-45	72	38	FLT	45	180	12	86															62	90	12	90				
				586.2	57.3	85.9	65	-35	87	55	fs	40	140	24	356															87	90	2	270				
				587.3	57.3	85.8	70	0	77	86	fs	23	-10	55	261															77	90	55	270				
				589.3	57.3	85.8	70	-40	84	48	f	60	145	37	29															82	90	20	90				
				589.8	57.4	85.7	35	-100	42	208	F	50	-45	76	232															23	270	72	270				
N28-99d	612.0	57.5	90.0																																		
				612.7	57.5	90.0	70	45	86	132																				85	90						
				618.0	57.5	90.1	68	20	81	109																				81	90						
				618.9	57.5	90.1	70	20	79	109	cqV	15	-65	41	249															79	90	39	270				
				620.4	57.6	90.1	63	17	86	105																				86	90						
				622.5	57.6	90.2	68	15	81	104																				80	90						
				624.0	57.6	90.2	68	10	80	100	FLT	30	150	16	339															80	90	6	270				
				626.0	57.6	90.2	80	35	73	126																				70	90						
				627.0	57.6	90.3	78	25	73	116																				71	90						
				629.0	57.6	90.3	73	15	76	105																				75	90						
				630.4	57.6	90.3	67	15	82	104																				81	90						
				631.0	57.6	90.3	75	20	74	110																				74	90						
				634.3	57.6	90.4	65	20	84	109																				84	90						
				636.0	57.7	90.4	85	22	65	115	F	50	110	47	351	F	40	120	35	346										63	90	10	270	9	270		
				636.3	57.7	90.4																															

			640.0	57.7	90.5					bx	55	-90	64	198												33	270		
			642.0	57.7	90.5	72	0	76	91	F/C	70	-90	75	190						FSlds	5	57	129	76	90	34	270		
642.0	57.7	90.5																											
			642.6	57.7	90.5	67	0	81	91															81	90				
			645.0	57.7	90.5	75	5	73	96															73	90				
			645.6	57.7	90.5	60	-5	88	86															88	90				
			646.4	57.7	90.5	75	5	73	96															73	90				
			647.2	57.8	90.5					FLT	23	-90	34	250												32	270		
			647.4	57.8	90.5	70	-90	75	190															34	270				
			647.8	57.8	90.5	78	25	73	116	F	35	-100	42	212										71	90	26	270		
			649.0	57.8	90.5	78	15	71	106															70	90				
			651.0	57.8	90.5	73	5	75	95															75	90				
			652.5	57.8	90.5	67	10	81	100															81	90				
			657.0	57.9	90.5	84	5	64	96															64	90				
			660.3	57.9	90.5	75	-10	73	80															73	90				
			663.0	57.9	90.5	80	-5	68	85															68	90				
			667.8	58.0	90.5	80	-10	68	80															68	90				
			669.0	58.0	90.5	80	-10	68	80															68	90				
			672.0	58.0	90.5	80	-10	68	80															68	90				
672.0	58.0	90.5																											
			676.0	58.0	90.4	84	-10	65	79															64	90				
			678.0	58.0	90.4	85	-10	64	79															63	90				
			679.5	58.0	90.4	87	-10	62	79															61	90				
			680.8	58.0	90.4					F	35	80	50	318												39	270		
			681.0	58.0	90.4	85	165	54	72															53	90				
			682.0	58.0	90.3	80	180	48	90															48	90				
			684.5	58.0	90.3	60	170	29	72															28	90				
			685.9	58.0	90.3					cV	30	125	28	332	cV	30	145	18	339							14	270	7	270
			686.0	58.0	90.3					cV	20	160	15	298	cV	40	160	14	26							13	270	6	90
			686.1	58.0	90.3					cV	35	150	17	358												1	270		
			686.7	58.0	90.3	72	-65	87	211	cV	30	180	2	270										84	270	2	270		
			687.3	58.0	90.2	65	-75	76	206	cV	30	-10	62	265										61	270	62	270		
			688.9	58.0	90.2					C/F?	45	165	16	48	cV	30	-10	62	265							12	90	62	270
			695.2	58.0	90.1	45	-160	18	142															11	90				
			696.0	58.0	90.1	45	-160	18	142	F	85	-90	86	183						FSlds	-60	2	273	11	90	33	270		
			696.5	58.0	90.1	42	-165	13	138															9	90				
			697.0	58.0	90.1	45	-170	14	120															13	90				
			698.1	58.0	90.1	45	-170	14	120															13	90				
			698.8	58.0	90.1	60	-155	33	132	FLT	75	110	67	9						FSlds	80	21	288	25	90	20	90		
			701.0	58.0	90.0	60	180	28	90															28	90				
			702.0	58.0	90.0	30	170	6	335															2	270				
702.0	58.0	90.0																											
			703.0	58.0	90.0	45	170	14	60	cV	70	-65	85	211										13	90	81	270		
			704.0	58.0	90.0	45	155	20	30															10	90				
			704.9	58.0	90.0	40	-165	12	144	F/SZ	25	165	10	309										7	90	8	270		
			705.4	58.0	90.0	60	-165	30	117															27	90				
			705.8	58.0	90.0	25	-160	12	225															8	270				
			706.1	58.0	90.0	50	-150	26	150															14	90				
			708.8	58.1	90.0	50	-155	24	142															15	90				
			710.0	58.1	90.0	60	-165	30	117															27	90				
			710.2	58.1	90.0					cV	65	-75	76	206												61	270		
			711.0	58.1	90.0	55	-155	28	137															20	90				
			712.5	58.1	90.0	56	-160	28	128															22	90				
			715.0	58.1	90.0	50	110	47	351															10	270				
			731.3	58.3	90.0					Styl$	20	-175	12	262												12	270		
			731.8	58.3	90.0	75	155	47	56	cV	70	-90	75	190						SSlds	80	41	265	42	90	32	270		
732.0	58.3	90.0																											
			732.4	58.3	90.0					F	72	-84	78	195						FSlds	-35	22	110			50	270		
			733.0	58.3	90.0	70	150	44	48	cV	70	-90	75	190										36	90	32	270		
			733.3	58.3	90.0					cl$	57	-110	52	183						cSlds	-10	31	121			4	270		
			733.7	58.3	90.0					F	75	-80	82	196						FSlds	-55	4	107			65	270		
			734.8	58.3	90.0	70	-170	39	105	F	65	-75	76	206	cV	60	-95	62	193	FSlds	60	59	272	38	90	61	270	23	270
			735.4	58.3	90.0	70	-160	41	119	F	55	-135	38	162	cV	66	-90	71	192	FSlds	80	27	211	37	90	14	90	32	270
			735.9	58.3	90.0					F	63	-45	87	231												86	270		
			737.9	58.4	90.0	60	180	28	90	F	70	-65	85	211						FSlds	-60	2	121	28	90	81	270		
			739.0	58.4	90.0	60	-170	29	108															28	90				
			742.0	58.4	90.0	67	170	36	74	cV	62	-65	78	215										35	90	70	270		
			744.3	58.4	90.0	60	160	32	56	cV	75	-75	85	200										27	90	76	270		
			746.0	58.5	90.0	58	165	28	62															26	90				
			747.0	58.5	90.0	57	165	27	62	cV	65	-85	71	198										25	90	42	270		
			751.0	58.5	90.0	64	60	35	60											SSlds	-20	35	56	31	90				
			755.3	58.6	90.0	75	60	47	60															42	90				
			757.2	58.6	90.0	65	60	36	60	cV	55	150	78	231										32	90	75	270		
			756.3	58.6	90.0	67	60	38	60											SSlds	-5	37	74	34	90				
			762.4	58.7	90.0	45	60	15	60	cV	55	-20	31	36						SSlds	10	13	93	13	90	20	90		
			764.1	58.7	90.0	55	170	25	70	cV	55	-20	85	254										23	90	85	270		

765.0	58.7	90.0																											
			765.5	58.7	90.0	47	170	17	64											SSlds	-20	17	62	15	90				
			770.0	58.8	90.0	50	60	21	60	cV1	75	-75	76	354	cV2	75	115	83	198	SSlds	25	14	107	18	90	25	270	69	270
			775.6	58.8	90.0	57	60	28	60											SSlds	80	4	337	25	90				
			777.9	58.8	90.0					bseF?	55		53	207												31	270		
			781.3	58.9	90.0					F	55		53	207						FSlds	-55	1	289			31	270		
			781.8	58.9	90.0		40			F	66		53	207						FSlds	-80	22	274			31	270		
			783.3	58.9	90.0	65	125	51	17															20	90				
			785.4	58.9	90.0	72	160	43	62	F	75	135	55	33						FSlds	-85	25	323	40	90	38	90		
			785.8	58.9	90.0	70	150	45	48															36	90				
			786.0	58.9	90.0	72	160	43	62															40	90				
			787.0	58.9	90.0	62	135	44	25															22	90				
			788.0	58.9	90.0	60	145	37	35	cV	60	-90	64	197										24	90	31	270		
			789.2	58.9	90.0	60	175	29	81	pycV	75	-60	88	33										29	90	87	90		
			789.4	58.9	90.0	60	180	29	90	FLT	65	-70	78	210						FSlds	20	75	169	29	90	67	270		
			790.7	59.0	90.0					FLT	50	145	29	25						FSlds	27	12	93			13	90		
			791.0	59.0	90.0	55	190	25	110															24	90				
			792.4	59.0	90.0	55	165	26	61															23	90				
			793.3	59.0	90.0	57	175	26	80	Jf	65	85	71	342						JSlds	5	48	50	26	90	42	270		
			795.0	59.0	90.0	55	165	26	61															23	90				
			796.8	59.0	90.0	60	155	34	49															27	90				
			799.0	59.0	90.0	60	180	29	90															29	90				
			801.0	59.1	90.0	60	175	29	81															29	90				
795.0	59.0	90.0																											

HOLE	SURVEY DATA Dpth	Plng	Dir	DPTH	PLNG	DIR	d	Dip Azim= 90	LOCAL S0 Dip	Dir	?	d	a	Sa Dip	Dir	?	d	a	Sb Dip	Dir	?	d	a	Sc Dip	Dir	?	B	La Plng	Dir	90 S0 Dip	Dir	90 Sa Dip	Dir	90 Sb Dip	Dir	90 Sc Dip	Dir
I22-55	0.0	90.0	270.0																																		
				24.0	89.5	274.5	20	90	20	90																				20	90						
				26.6	89.5	275.0	21	90	21	90	mf	60	140	60	230															21	90	52	270				
				31.2	89.4	275.9	10	90	11	90	mf	58	105	58	194															11	90	21	270				
				39.7	89.3	277.5	9	90	10	90	mf	70	110	70	199															10	90	42	270				
				45.0	89.2	278.5	10	90	11	90	mf	65	85	65	174															11	90	13	90				
				47.7	89.1	279.0	18	90	19	90																				19	90						
				52.0	89.0	279.8	14	90	15	90																				15	90						
	53.0	89.0	280.0																																		
				53.6	89.0	279.5	12	90'	13	90																				13	90						
				58.5	88.6	275.3	13	90	14	90	V	87	-130	86	320															14	90	84	270				
	60.0	88.5	274.0																																		
				63.0	88.5	273.0	17	90	19	90																				19	90						
				65.9	88.4	272.1	25	90	27	90																				27	90						
				70.3	88.4	270.7	18	90	20	90																				20	90						
				71.6	88.4	270.3	45	90	47	90																				47	90						
				72.5	88.4	270.0	35	90	37	90																				37	90						
				80.0	88.3	267.6	18	90	20	90																				20	90						
				82.4	88.2	266.9	18	90	20	90																				20	90						
				85.1	88.2	266.0	7	90	9	90																				9	90						
				86.3	88.2	265.6	23	90	25	90	V	75	-140	74	311															25	90	69	270				
				94.3	88.1	263.1	13	90	15	90																				15	90						
				95.5	88.1	262.7	16	90	18	90																				18	90						
				96.1	88.1	262.5	5	90	7	90	V	80	120	79	213															7	90	70	270				
				98.7	88.1	261.7	14	90	16	90	V	85	55	86	146															16	90	83	90				
	104.0	88.0	260.0																																		
				114.9	88.0	262.3	15	90	17	90																				17	90						
				118.0	88.0	263.0	12	90	14	90	VF	75	-95	75	357															14	90	12	270				
				119.7	88.0	263.4	14	90	16	90																				16	90						
				128.8	88.0	265.3	15	90	17	90																				17	90						
				134.5	88.0	266.5	14	90	16	90	cEV	76	-20	78	71															16	90	77	90				
				135.4	88.0	266.7	8	90	10	90																				10	90						
				132.8	88.0	266.2	10	90	12	90	T	30	10	32	100															12	90	32	90				
				136.6	88.0	267.0	6	90	8	90																				8	90						
				137.5	88.0	267.2	14	90	16	90																				16	90						
				137.9	88.0	267.3	5	90	7	90																				7	90						
				139.0	88.0	267.5	10	90	12	90	V1	90	65	89	336	V2	90	-20	88	250										12	90	88	270	88	270		
				140.1	88.0	267.7	11	90	13	90	T	40	-75	41	18	sgV	90	-130	89	320										13	90	15	90	88	270		
				141.1	88.0	268.0	12	90	14	90	F	27	-35	29	57															14	90	25	90				
				141.7	88.0	268.1	5	90	7	90																				7	90						
				142.5	88.0	268.3	6	90	8	90	E	27	0	29	90															8	90	29	90				
				142.2	88.0	268.2	11	90	13	90																				13	90						
				143.1	88.0	268.4	11	90	13	90	E	27	-20	29	71															13	90	28	90				
				145.3	88.0	268.9	7	90	9	90																				9	90						
				145.6	88.0	268.9	12	90	14	90	T	10	-170	8	283															14	90	8	270				
				146.5	88.0	269.1	8	90	10	90	E	28	-115	27	339	E	24	95	24	181										10	90	11	270	0	270		
				147.1	88.0	269.2	6	90	8	90	Emf	47	-5	49	85															8	90	49	90				
				148.0	88.0	269.4	8	90	10	90	E	25	-140	24	313	T	40	-55	41	37										10	90	18	270	28	90		
				148.6	88.0	269.6	17	90	19	90	T	26	-135	25	318															19	90	17	270				
				148.8	88.0	269.6	7	90	9	90	T	65	30	67	120	sgV	77	65	78	155										9	90	64	90	63	90		
				150.0	88.0	269.9	17	90	19	90	sgV	80	85	80	175															19	90	28	90				
				151.4	88.0	270.2	5	90	7	90																				7	90						
				151.6	88.0	270.2	9	90	11	90	E	52	13	54	103															11	90	53	90				
				152.0	88.0	270.3	7	90	9	90																				9	90						
				152.3	88.0	270.4	11	90	13	90	E	45	5	47	95															13	90	47	90				
				152.7	88.0	270.4	9	90	11	90	TR	27	-45	28	48															11	90	22	90				
				152.9	88.0	270.5	10	90	12	90	Emf	47	10	49	100															12	90	49	90				
	153.0	88.0	270.5																																		
				157.5	88.0	270.3	6	90	8	90																				8	90						
				158.3	88.0	270.2	13	90	15	90	T	7	-160	5	297	S02	5	-15	7	79										15	90	5	270	7	90		
				158.1	88.0	270.2	12	90	14	90	mf	40	-145	38	306	Ef	10	-145	8	313										14	90	33	270	6	270		
				159.0	88.0	270.2	13	90	15	90	T	23	120	22	206	S02	11	55	12	137										15	90	10	270	8	90		
				159.2	88.0	270.2	14	90	16	90	T	12	-120	11	339															16	90	4	270				
				159.7	88.0	270.2	7	90	9	90	T	10	140	9	221															9	90	6	270				
				160.2	88.0	270.1	8	90	10	90																				10	90						
				160.7	88.0	270.1	9	90	11	90	T	5	-100	5	13															11	90	1	90				
				160.8	88.0	270.1	9	90	11	90	T	5	-135	4	336															11	90	2	270				
				161.4	88.0	270.1	10	90	12	90																				12	90						
				161.7	88.0	270.0	10	90	12	90	V	85	50	86	140															12	90	84	90				
				166.7	88.0	269.8	22	90	24	90																				24	90						
				190.4	88.0	268.6	12	90	14	90																				14	90						
				191.3	88.0	268.5	10	90	12	90																				12	90						
				193.1	88.0	268.4	10	90	12	90																				12	90						
				194.9	88.0	268.3	12	90	14	90																				14	90						

			195.3	88.0	268.3	10	90	12	90											12	90				
201.0	88.0	268.0																							
			203.7	88.0	267.5	7	90	9	90											9	90				
			207.7	88.0	266.8	13	90	15	90											15	90				
			210.0	88.0	266.4	10	90	12	90	mf	65	170	63	261						12	90	63	270		
			217.0	88.0	265.1	10	90	12	90	mf	35	145	33	234						12	90	28	270		
			217.9	88.0	265.0	13	90	15	90	mf	56	160	54	250						15	90	52	270		
			219.2	88.0	264.7	11	90	13	90	mf	56	145	54	235						13	90	49	270		
			223.5	88.0	264.0	12	90	14	90	mf	43	165	41	256						14	90	40	270		
			230.9	88.0	262.6	9	90	11	90	mf	30	100	29	188						11	90	5	270		
			235.1	88.0	261.9	10	90	12	90	mf	45	150	43	241	V	85	40	86	131	12	90	39	270	85	90
			237.8	88.0	261.4	10	90	12	90	mf	62	160	60	252						12	90	59	270		
			245.3	88.0	260.0	11	90	13	90	mf	45	150	43	241						13	90	39	270		
			250.4	88.0	259.1	10	90'	12	90											12	90				
251.0	88.0	259.0																							
			259.3	87.9	259.3	13	90	15	90	mf	60	170	58	262						15	90	58	270		
			266.7	87.8	259.6	15	90	17	90	mf	64	145	62	236						17	90	57	270		
			271.8	87.8	259.8	13	90	15	90	mf	70	110	69	201						15	90	43	270		
			273.8	87.8	259.9	8	90	10	90	mf	63	135	61	227	V	80	-150	78	303	10	90	53	270	76	270
			274.5	87.8	259.9	20	90	22	90											22	90				
			275.0	87.8	260.0	23	90	25	90											25	90				
			275.4	87.8	260.0	55	90	57	90											57	90				
			275.9	87.7	260.0	80	90	82	90	f	45	15	47	104						82	90	46	90		
			276.0	87.7	260.0	80	90	82	90	FAULT	63	175	61	265						82	90	61	270		
			276.7	87.7	260.0	73	90	75	90	F	32	0	34	90						75	90	34	90		
			276.4	87.7	260.0	90	90	88	270											88	270				
			276.9	87.7	260.0	60	90	62	90											62	90				
			277.1	87.7	260.1	45	90	47	90											47	90				
			277.2	87.7	260.1	45	90	47	90											47	90				
			277.7	87.7	260.1	17	90	19	90	F	66	-120	65	332						19	90	45	270		
			282.0	87.7	260.3	14	90	16	90	cEVs	85	-60	87	32						16	90	83	90		
			283.5	87.7	260.3	12	90	14	90	mf	62	135	60	226						14	90	51	270		
			285.5	87.7	260.4	11	90	13	90											13	90				
			289.8	87.6	260.6	10	90	12	90	mf	60	150	58	242						12	90	54	270		
			291.4	87.6	260.6	10	90	12	90	mf	62	160	60	252						12	90	58	270		
			294.0	87.6	260.7	20	90	22	90											22	90				
			309.0	87.4	261.3	20	90	23	90											23	90				
			313.0	87.4	261.5	27	90	30	90											30	90				
			318.0	87.3	261.7	25	90	28	90											28	90				
			321.5	87.3	261.8	23	90	26	90											26	90				
			323.0	87.3	261.9	65	90	68	90	cVs	25	180	22	271						68	90				
			323.6	87.3	261.9	80	90	83	90											83	90				
			324.6	87.3	262.0	30																			
			324.1	87.3	262.0	45																			
			331.0	87.2	262.2	40	90	43	90											43	90				
			332.0	87.2	262.3	30	90	33	90											33	90				
			334.0	87.2	262.4	15	90	18	90	cV1	60	120	58	210	cV2	85	-170	82	282	18	90	39	270	82	270
			341.5	87.1	262.7	40	90	43	90											43	90				
			348.0	87.0	262.9	80	90	83	90											83	90				
350.0	87.0	263.0																							
			352.0	87.0	262.7	60	90	63	90											63	90				
			354.2	87.0	262.4	70																			
			355.7	87.0	262.2	45	90	48	90											48	90				
			365.0	87.0	260.9	50	90	53	90											53	90				
			371.5	87.0	260.0	25	90	28	90											28	90				
			385.0	87.0	258.1	25	90	28	90											28	90				
			394.0	87.0	256.8	20	90	23	90											23	90				
			401.0	87.0	255.9	33	90	36	90											36	90				
400.0	87.0	256.0																							

HOLE	SURVEY DATA Dpth	Plng	Dir	DPTH	PLNG	DIR	d	Dip Azim= 85	LOCAL S0 Dip	Dir	?	d	a	Sa Dip	Dir	?	d	a	Sb Dip	Dir	?	d	a	Sn Dip	Dir	?	B	La Plng	Dir	90 S0 Dip	Dir	90 Sa Dip	Dir	90 Sb Dip	Dir	90 Sc Dip	Dir
K22-55W	0.0	80.0	265.0																																		
				171.2	80.0	267.7	11	85	21	85	f	53	-90	53	360															21	90	0	270				
				174.5	80.0	267.8	30	85	40	85	mf	55	160	46	241	Tf	20	160	11	224										40	90	42	270	8	270		
				175.0	80.0	267.8	32	85	42	85	mf	40	135	34	208															42	90	18	270				
				175.8	80.0	267.8	20	85	30	85	F.	47	125	42	199															30	90	17	270				
				176.6	80.0	267.8	12	85	22	85																				22	90						
				176.8	80.0	267.8	12	85	22	85	mf	42	180	32	261															22	90	32	270				
				177.6	80.0	267.8	8	85	18	85																				18	90						
				180.0	80.0	267.9	7	85	17	85																				17	90						
				180.3	80.0	267.9	7	85	17	85	Ef	32	0	42	82															17	90	41	90				
				182.2	80.0	267.9	30	85	40	85																				40	90						
				183.8	80.0	267.9	10	85	20	85																				20	90						
				183.6	80.0	267.9	10	85	20	85	T	37	0	47	83															20	90	47	90				
				184.3	80.0	267.9	7	85	17	85	IT	8	-170	2	83															17	90	2	90				
				184.4	80.0	267.9	10	85	20	85	T	18	-130	12	344	T	12	180	2	229	T	30	-80	32	17					20	90	3	270	1	270	10	90
				185.5	80.0	267.9	6	85	16	85	f	38	80	42	148															15	90	25	90				
				185.7	80.0	267.9	7	85	17	85	Ef	18	175	8	240															17	90	7	270				
				186.1	80.0	268.0	7	85	17	85	Ef	30	10	40	89															17	90	40	90				
				186.6	80.0	268.0	7	85	17	85	?	15	-50	22	52															17	90	17	90				
				187.4	80.0	268.0	7	85	17	85	Ef	40	-25	48	60															17	90	44	90				
	189.0	80.0	268.0																																		
				189.3	80.0	268.0	6	85	16	85	T	13	170	4	203	ER	18	0	28	82										15	90	2	270	27	90		
				189.4	80.0	268.0	7	85	17	85	T	33	10	43	89															17	90	43	90				
				190.1	80.0	268.1	11	85	21	85	T	25	125	22	184															21	90	2	270				
				190.3	80.0	268.1	10	85	20	85	T	15	130	12	169	Ef	38	-20	47	66										20	90	2	90	44	90		
				191.0	80.0	268.1	6	85	16	85	Ef	30	0	40	81															16	90	39	90				
				191.2	80.0	268.1	7	85	17	85	f	25	-110	22	352															17	90	3	270				
				192.6	80.0	268.2	11	85	21	85	T	27	80	31	145	V	70	0	80	82										21	90	19	90	80	90		
				192.9	80.0	268.2	8	85	18	85	TR	32	0	42	82															18	90	41	90				
				193.2	80.0	268.2	11	85	21	85	V	78	0	88	82															21	90	88	90				
				194.6	80.0	268.3	6	85	16	85	V	85	-10	86	248															16	90	85	270				
				195.9	79.9	268.4	6	85	16	85	Ef	57	-75	58	9															16	90	14	90				
				196.2	79.9	268.4	5	85	15	85	Ef	34	-20	43	63	TR	5	-140	7	68										15	90	39	90	6	90		
				197.0	79.9	268.4	5	85	15	85	Ef	32	-25	40	59															15	90	36	90				
				197.3	79.9	268.4	11	85	21	85	T	32	-30	40	59															21	90	36	90				
				197.4	79.9	268.4	10	85	20	85	V	87	-30	85	231															20	90	84	270				
				203.5	79.9	268.8	5	85	15	85	T	33	-45	39	42															15	90	28	90				
				204.3	79.9	268.8	10	85	20	85	Ef1	42	-75	44	16	Ef2	25	170	15	240										20	90	14	90	13	270		
				204.8	79.9	268.8	7	85	17	85	Ef	38	-35	45	51															17	90	38	90				
				204.7	79.9	268.8	10	85	20	85	mf1	70	170	60	249	Ef2	35	-115	30	340										20	90	59	270	11	270		
				205.0	79.9	268.8	10	85	20	85																				20	90						
				206.0	79.9	268.9	9	85	19	85	V	77	95	78	173															19	90	31	90				
				206.4	79.8	268.9	8	85	18	85	Tf	50	130	45	201	V	80	35	89	114										18	90	20	270	89	90		
				208.2	79.8	269.0	3	85	13	85																				13	90						
				211.9	79.8	269.2	5	85	15	85	psgV	70	-75	70	3															15	90	8	90				
				212.4	79.8	269.2	8	85	18	85	TF	20	145	14	194															18	90	4	270				
				239.3	79.6	270.6	14	85	24	85																				24	90						
				239.8	79.6	270.7	9	85	19	85																				19	90						
				240.4	79.5	270.7	10	85	20	85																				20	90						
				243.0	79.5	270.8	16	85	26	85																				26	90						
				244.0	79.5	270.9	27	85	37	85																				37	90						
				246.2	79.5	271.0	5	85	15	85																				15	90						
				246.5	79.5	271.0	13	85	23	85	Ef	75	-20	84	61	V	85	-5	85	255										23	90	83	90	85	270		
				246.6	79.5	271.0	21	85	31	85	Ef	68	-45	74	40	V	80	-20	89	62										31	90	66	90	89	90		
	246.0	79.5	271.0																																		

HOLE	SURVEY DATA Dpth	Plng	Dir	DPTH	PLNG	DIR	d		DipAz	LOCAL S0 Dip	Dir	?	d		a	Sa Dip	Dir	?	d	(C/O) a	ADJ (C/O) a	Sb Dip	Dir	?	d	(C/O) a	ADJ (C/O) a	Sc Dip	Dir	?	B	La Plng	Dir	90 S0 Dip	Dir	90 Sa Dip	Dir	90 Sb Dip	Dir	90 Sc Dip	Dir
R29-05	0.0	90.0	255.0																																						
				18.0	89.7	255.2	85																																		
				32.5	89.5	255.3	88																																		
				40.1	89.3	255.4	90																																		
				43.0	89.3	255.4	87																																		
				44.9	89.3	255.5	50																																		
				82.5	88.6	255.9	35																																		
				91.2	88.5	256.0	60																																		
				104.0	88.3	256.1	55	-160	151	53	226																							44	270						
				108.0	88.2	256.1	65	-160	151	63	227																							56	270						
				118.2	88.0	256.2	57	-160	151	55	227																							46	270						
				119.5	88.0	256.2	55	-160	151	53	227																							44	270						
				132.6	87.8	256.4						f	55	0	-49	56	29																			36	90				
				141.0	87.7	256.5	48	-160	151	46	226																							37	270						
				151.0	87.5	256.6	55	-160	151	53	227																							44	270						
				156.5	87.4	256.6	65	-160	151	63	227																							55	270						
				157.3	87.4	256.6	65	-160	151	63	227																							55	270						
				166.7	87.2	256.7	85	-180	131	83	208																							75	270						
				172.1	87.1	256.8	85	0	-49	87	28																							83	90						
				172.3	87.1	256.8						TF????	45	180	131	43	206																			22	270				
				172.5	87.1	256.8	40	-130	-179	37	258																			SSlds	-25	33	227	37	270						
				174.1	87.1	256.8	72	-160	151	69	227																							63	270						
				174.9	87.1	256.8	70	-100	-149	68	288																							66	270						
				176.0	87.1	256.8	90	80	31	87	288																							87	270						
				176.1	87.1	256.8	70	80	31	73	107																							72	90						
				176.3	87.1	256.8	88	90	41	90	298																							90	270						
				177.0	87.1	256.8	55	80	31	58	107																							56	90						
				177.1	87.0	256.8	90	80	31	87	288																							87	270						
				177.4	87.0	256.8	90	55	6	87	263																							87	270						
				179.0	87.0	256.9	87	25	-24	90	53																							90	90						
				179.8	87.0	256.9	55	100	51	57	126																							51	90						
				180.0	87.0	256.9	55	100	51	57	126																							51	90						
				181.0	87.0	256.9	40	100	51	42	125																							36	90						
				181.5	87.0	256.9						TFLT	35	50	1	38	78													FSlds	-10	37	65			37	90				
				182.2	87.0	256.9	88	-20	-69	89	8																							83	90						
				183.0	87.0	256.9	87	-10	-59	89	18																							85	90						
				184.0	86.9	256.9	43	150	101	43	175																							5	90						
				184.9	86.9	256.9	50	175	126	48	201																							22	270						
				185.5	86.9	256.9	42	130	81	43	155																							22	90						
				186.7	86.9	256.9	44	150	101	43	175																							5	90						
				187.5	86.9	257.0	37	170	130	35	204																							16	270						
				188.5	86.9	257.0	42	180	140	40	215																							25	270						
				189.3	86.8	257.0	50	150	110	49	184																							5	270						
				189.4	86.8	257.0						SOTF	55	-170	150	52	226													SSlds	20	47	259			43	270				
				189.5	86.8	257.0	75	-175	145	72	221																							64	270						
				190.8	86.8	257.0	80	180	140	78	217																							70	270						
				191.1	86.8	257.0	80	0	-40	82	37																							78	90						
				191.2	86.8	257.0	75	180	140	73	216																							62	270						
				191.5	86.8	257.0	73	180	140	71	216																							59	270						
				192.5	86.8	257.0	68	-170	150	65	226																							57	270						
				193.0	86.8	257.0	70	180	140	68	216																							55	270						
				193.4	86.8	257.0						TFLT	60	70	30	63	106																			62	90				
				193.6	86.8	257.0						TFLT	62	75	35	65	111																			63	90				
				194.0	86.8	257.0	65	180	140	63	216																							49	270						
				195.0	86.8	257.0	73	180	140	71	216																							59	270						
				196.0	86.7	257.0	75	0	120	73	196	TFLT	20	170	-70	21	15																	43	270	6	90				
				196.4	86.7	257.0						TFLT	25	0	120	24	191																			5	270				
				196.5	86.7	257.0	50	15	135	48	210																							29	270						
				197.6	86.7	257.1	65	-80	133	63	209																							43	270						
				197.7	86.7	257.1						TFLT	65	-80	133	63	209																			43	270				
				198.5	86.7	257.1	75	-80	133	73	209																							58	270						
				199.2	86.7	257.1	80	-95	118	78	195																							51	270						
				200.2	86.7	257.1	62	80	-67	63	12																							22	90						
				200.5	86.7	257.1	75	175	28	78	105																							78	90						
				201.4	86.6	257.1	64	-140	73	65	149																							48	90						
				201.6	86.6	257.1	40	-30	-177	37	260																							36	270						
				201.7	86.6	257.1	60	60	-87	60	352																							14	270						
				202.1	86.6	257.1	90	90	-57	88	200																							85	270						
				202.5	86.6	257.1	88	0	-57	90	20																							90	90						
				202.8	86.6	257.1	88	0	-57	90	20	F	55	15	-42	58	37																	90	90	43	90				
				203.0	86.6	257.1	55	15	-42	58	37																							43	90						
				206.4	86.6	257.2	77		-50	79	28																							68	90						
				210.0	86.5	257.2	78	0	120	76	196																							49	270						
				210.2	86.5	257.2	80	180	-60	82	18																							65	90						
				211.7	86.5	257.2	85	0	120	83	197																							68	270						
				213.1	86.4	257.2	70	-150	-30	73	48																							68	90						

	216.0	86.4	257.3						2f	40	-90	30	43	105													42	90		
	216.3	86.4	257.3						T	55	-150	-30	58	48													50	90		
	216.4	86.4	257.3						T	55	-165	-45	58	34													41	90		
	216.5	86.4	257.3						T	47	-155	-35	50	44													40	90		
	216.6	86.4	257.3						T	60	-155	-35	63	43													51	90		
	219.9	86.3	257.3	55		0	59	77																	58	90				
	220.0	86.3	257.3	70		0	74	77																	73	90				
	222.9	86.3	257.3	77		0	81	77																	80	90				
	224.0	86.3	257.3	84		0	88	77																	88	90				
	224.9	86.3	257.3	85		0	89	77																	89	90				
	229.5	86.2	257.4	82		0	86	77																	86	90				
	236.1	86.1	257.5	85	0	0	89	77																	89	90				
	236.2	86.1	257.5						FLT	72	100	100	71	176													11	90		
	236.2	86.1	257.5						FLT	65	120	120	63	196													28	270		
	237.6	86.0	257.5	50		0	54	77																	53	90				
	250.4	85.8	257.6	70		0	74	78																	74	90				
	257.0	85.7	257.7	77		0	81	78																	81	90				
	266.0	85.6	257.8	77		0	81	78																	81	90				
	266.8	85.6	257.8	75		0	79	78																	79	90				
	269.1	85.5	257.8	70		0	74	78																	74	90				
	269.3	85.5	257.8	55		0	59	78																	59	90				
	276.2	85.4	257.9	68		0	73	78																	72	90				
	277.2	85.4	257.9	60	0	0	65	78																	64	90				
	277.3	85.4	257.9	90	0	0	85	258																	85	270				
	277.3	85.4	257.9	60	180	-180	55	258																	55	270				
	277.4	85.4	257.9	90	0	0	85	258																	85	270				
	279.1	85.3	257.9	50		0	55	78																	54	90				
	279.6	85.3	257.9	50		0	55	78																	54	90				
	280.5	85.3	257.9	60		0	65	78																	64	90				
	295.5	85.1	258.1	20		0	25	78																	24	90				
	296.8	85.1	258.1	68		0	73	78	TP	30	0	0	35	78											73	90	34	90		
	300.5	85.0	258.1	28		0	33	78																	32	90				
	304.5	84.9	258.2	15		0	20	78																	20	90				
	309.7	84.8	258.2	10		0	15	78																	15	90				
	312.9	84.8	258.3	45		0	50	78																	50	90				
	313.5	84.8	258.3	90		0	85	258																	85	270				
	313.9	84.8	258.3	70		0	75	78																	75	90				
	314.8	84.8	258.3	85		0	90	258																	90	270				
	315.7	84.7	258.3						TFLT	25		0	30	78											0	90	30	90		
	318.0	84.7	258.3	17		0	22	78																	22	90				
	321.5	84.6	258.3	30		0	35	78																	35	90				
	325.6	84.6	258.4	28		0	33	78																	33	90				
	328.7	84.5	258.4	35		0	40	78																	40	90				
	336.4	84.4	258.5	60		0	66	79																	65	90				
	357.5	84.0	258.7	28		0	34	79																	33	90				
	360.5	84.0	258.8	50		0	56	79																	55	90				
	388.0	83.5	259.0	50		0	56	79																	56	90				
	424.3	82.9	259.4	40		0	47	79																	47	90				
	442.9	82.6	259.6	30	-120	-120	27	332																	13	270				
	443.1	82.6	259.6	45	-90	-90	43	358																	2	270				
	443.5	82.6	259.6	75	-100	-100	74	342																	47	270				
	443.9	82.6	259.6						TF	33	70	70	36	140													25	90		
	444.3	82.6	259.6	57	0	0	64	80	T	27	60	60	31	129											64	90	25	90		
	445.4	82.6	259.6	44		0	51	80																	51	90				
	450.0	82.5	259.7	55		0	63	80																	62	90				
	450.4	82.5	259.7	42		0	50	80																	49	90				
	452.0	82.5	259.7	35		0	43	80																	42	90				
	454.8	82.4	259.7	35		0	43	80																	42	90				
	461.0	82.3	259.8	44		0	52	80																	51	90				
	466.3	82.2	259.9	30		0	38	80																	37	90				
	466.9	82.2	259.9	32		0	40	80																	39	90				
R29-05b	470.8	82.2	259.9	40	180	-30	47	54	SOF	40	180	-30	47	54											41	90	41	90		
	471.0	82.2	259.9	45	180	-30	52	53	SOF	45	180	-30	52	53											46	90	46	90		
	471.1	82.1	259.9	52	180	-30	59	53																	53	90				
	471.3	82.1	259.9	45	180	-30	52	53																	46	90				
	471.5	82.1	259.9	45	180	-30	52	53	F	62	-150	0	70	80	F	60	-110	40	66	117					46	90	70	90	64	90
	471.8	82.1	259.9	45	180	-30	52	53	SOF	45	180	-30	52	53											46	90	46	90		
	472.1	82.1	259.9	52	180	-30	59	53	F	68	-130	20	75	99											53	90	75	90		
	472.5	82.1	259.9	40	150	-60	44	27	SOF	40	150	-60	44	27							sslds	15	44	34	24	90	24	90		
	473.5	82.1	259.9	60	160	-50	65	33	fa	90	30	-180	82	260											50	90	82	270		
	474.5	82.1	259.9	90	180	-30	83	230																	81	270				
	474.6	82.1	259.9						FLT	80	-130	20	84	21													74	90		
	474.8	82.1	259.9	80	180	-30	87	50	T	33	-120	30	40	105											86	90	39	90		
	474.9	82.1	259.9	65	180	-30	72	51																	67	90				
	475.0	82.1	259.9	67	180	-30	74	51	T	25	180	-30	32	57											70	90	28	90		
	475.5	82.1	260.0	57	170	-40	63	43																	53	90				
	476.0	82.1	260.0	60		0	68	80																	68	90				
	477.0	82.1	260.0	44		0	52	80																	52	90				
	479.0	82.0	260.0	45		0	53	80																	53	90				
	480.0	82.0	260.0																											